Energy Equip. Sys./ Vol. 12/No. 4/December 2024/ 285-326

ENERGY EQUIPSYS

Energy Equipment and Systems

www.energyequipsys.com

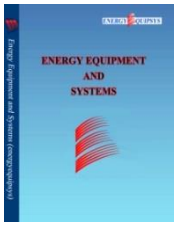

Analysis of the effect of coating the piston crown with ceramic material on the mechanical behavior of four-cylinder diesel engine components using the finite element method

Manuscript Type
Research Paper

Authors

Seyyed Amirreza Abdollahi[a*]
Seyyed Faramarz Ranjbar[a]
Mohammad Babaei Parvazian[a]
Nasim sahaf amin[a]
Mahsa Jodeiri Feizi[b]
Sana Sahaf Amin[a]

[a] Faculty of Mechanical Engineering, University of Tabriz, Tabriz, Iran

[b] Polytechnic Milan Italy/Piacenza 20156.

Article history:

Received : 15 December 2023
Revised :17 March 2024
Accepted : 3 April 2024

ABSTRACT

With the invention of internal combustion engines in the late 19th century, a tremendous transformation in the field of transportation occurred, paving the way for acceleration in all human endeavors. Consequently, internal combustion engines have continuously advanced, with industry players competing and innovating in this sector. Various industries have shown a noticeable interest in creative approaches to design and improve the quality and performance of these engines. Internal combustion engines can be broadly categorized into gasoline and diesel engines. Marine diesel engines, like gasoline engines, are internal combustion or internal ignition engines that convert chemical energy from fuel into thermal energy inside the cylinder and then convert thermal energy into the mechanical energy required for ignition generation. The importance and necessity of using diesel engines in various industries, especially in maritime applications, are undeniable, as the focus of this research. The field of diesel engines is considered one of the crucial components of a country's industrial and scientific self-reliance and ignition, with the measurement of a nation's capacity and ignition in various sectors, from politics and economics to defense and military, being dependent on the knowledge, analysis, design, and production of equipment and tools that are internationally competitive. Key parameters that play a significant role in selecting engines include size, ignition, and how they perform in various applications. An engine's ignition level and appropriate performance are directly related to optimal design and understanding the forces and stresses applied to the engine components during operation. The primary objective of this project is to perform a mechanical analysis of the piston, connecting rod, and crankshaft in a 150-horse-ignition marine diesel engine, to improve thermal performance and enhance engine efficiency. To achieve this, an in-depth study will be conducted, using available diagrams to analyze these components, and the results obtained will be used to evaluate strategies for reducing thermal stresses and increasing efficiency. Ultimately, based on the research data, it can be concluded that the quenching process on the piston crown with a ceramic material reduces the maximum stress by an average of 40% for the critical element in four phases: compression, combustion, and exhaust. As a result, it increases the reliability coefficient by 23% for the critical element in the ignition phase.

Keywords: Stress, Strain, Diesel Engine, Thermal Stress, Coating.

[*] Corresponding author: Seyyed Amirreza Abdollahi
Faculty of Mechanical Engineering, University of Tabriz, Tabriz, Iran
E-mail address: s.a_abdollahi@yahoo.com

1. Introduction

Today, engine manufacturing is considered the foundation of industrial development in various countries, and engines serve as a prime source of energy production and conversion in any nation. An overview of the global expansion of internal combustion engines reveals that diesel engines, with different ignition capacities, have played a significant role during various periods compared to gasoline engines in terms of utilizing chemical fuel energy for mechanical work. Diesel engines are approximately 30% more fuel-efficient than gasoline engines, and the global cost of diesel fuel production is 10% lower than gasoline. Some of the factors that make diesel engines more popular compared to gasoline engines include the ability to use heavier fuels, increased specific ignition, the use of various supercharging methods, combination with gas turbines, lower pollution compared to gasoline engines, and longer maintenance and service intervals. Additionally, the growth of lightweight diesel engines has been on the rise in recent decades, relying on supercharging systems and turbocharging, resulting in a significant increase in ignition within a fixed engine volume.

A diesel engine is a type of internal combustion engine that utilizes the Diesel cycle to create motion. The main difference between diesel engines and other engines is the use of compression ignition. In these engines, an explosion does not occur; rather, the fuel and air mixture is highly compressed, causing it to ignite without sparking. The main rotation speed of these engines, unlike gasoline engines, is about 100 revolutions per minute. Diesel engines use diesel fuel, and the fundamental operation of all of them is the same.

Diesel engines can be categorized based on the number of combustion cycles per revolution of the crankshaft, the ignition output expressed in horse ignition, the number of cylinders, and the arrangement of the cylinders. Today, due to the need for reduced weight, high-output ignition, and low pollution, the components of diesel engines are subject to severe mechanical and thermal loads. Among the engine's essential internal components and its framework, key elements include the cylinder, cylinder head, connecting rod, piston, bushing, piston pin, piston rings, valves, and oil pump. The analysis and design of the engine are influenced by various mechanical loads acting on each of these components. Therefore, understanding the forces and stresses applied to each component can significantly contribute to the optimal and efficient design of diesel engines for various applications.

Given the importance of diesel engine technology and the need for improved performance, increasing ignition, and torque, and reducing fuel consumption, the application of modern materials in engine components is essential. Enhancing the performance of internal combustion engines, such as increasing ignition and torque while decreasing fuel consumption, is a significant challenge in the field of engine development. Improvements in engine performance require various tests and come with significant economic costs, human resources, and time investments. In the past, many experiments on engines were conducted empirically in well-equipped laboratories. However, at present, numerical methods based on finite element analysis and computer simulations have become valuable tools for optimizing engine design, reducing production costs, and obtaining results without the need for expensive experiments. Therefore, this research also employs theoretical principles and numerical methods using data and experimental measurements to analyze the piston, connecting rod, and crankshaft components in a Mercury Marine diesel engine.

2. Theoretical Foundations

2.1. Diesel Engines

The term "diesel" is derived from the name of a German inventor and engineer, Rudolf Diesel, who, after fourteen years of relentless work, patented a specific type of internal combustion engine in 1892. In his honor, these engines are referred to as diesel engines. Diesel engines encompass a wide range of engines that can ignite a combustible substance without the need for an electric spark. These engines use high temperatures to ignite the fuel, whereby the intake air temperature is significantly elevated, and after reaching the desired temperature, the fuel is mixed with air. The combustion of a fuel requires two essential elements: heat and oxygen. Oxygen enters the engine cylinder through the intake channels

and is then compressed by the piston. The compression is so intense that it generates very high heat. Subsequently, the third element, the combustible substance, is added to the heat and oxygen, resulting in the ignition of the fuel.

The structural design of diesel engines differs from spark-ignition engines only in the fuel delivery and regulation system. In a diesel engine, pure air is compressed inside the engine cylinder. To prevent premature ignition, fuel is injected into the compressed air. The injected fuel self-ignites due to the high pressure and temperature, and as long as fuel injection continues, the combustion process persists. Hence, diesel engines are also known as compression-ignition engines. Understanding the main phases of operation is essential for comprehending the mechanism of a diesel engine, which is crucial for the design and analysis of engine components. In addition to design knowledge, mastery of the functioning of components and the forces acting on each component are vital for the construction and analysis of engine parts. The four main operations of a diesel engine include intake (breathing), compression (pressure), combustion (explosion), and exhaust.

Different parts of marine diesel engines are categorized into two main groups: moving parts and stationary parts. The moving parts of engines include the piston, pistons, piston rings, piston pins, valves, crankshaft, connecting rod, and more. On the other hand, the stationary parts of marine diesel engines include the cylinder block, cylinder head, and so on. In general, to achieve maximum efficiency and performance in marine diesel engines, understanding the nature and function of each engine component, conducting mechanical analysis of engine parts, and ensuring proper manufacturing of components are essential and unavoidable tasks.

2.2. Mercury Marine engine

The Mercury Marine engine is used in marine propulsion, primarily in sea-going vessels such as boats and ships. These diesel engines utilize state-of-the-art technology to maximize their performance and increase the longevity of their components. They feature advanced anti-corrosion systems, including a closed-loop cooling system with a thermostat. In this engine, motor oil, gear oil, and ignition steering oil are cooled with water, which helps reduce the engine's temperature. Additionally, it incorporates the SeaCore® system for ultimate protection against saltwater. The high-pressure common rail fuel injection system not only ensures fuel efficiency but also minimizes noise, vibration, and harshness (NVH) along with reducing emissions. The lightweight and compact design of these diesel engines makes them ideal replacements for many older, fuel-hungry gasoline engines, providing significant acceleration and quick throttle response through the common rail fuel injection system.

2.3. Research Background

The research background focuses on internal combustion engines, which are engines where a fuel-air mixture ignites within a closed chamber to generate ignition [1]. During the combustion process, high-temperature and high-pressure gases are produced, causing moving engine components to generate motion, thus producing ignition. Generating ignition in diesel engines is associated with the application of forces and stresses to the engine's components. Therefore, understanding and analyzing these stresses in engine design is crucial depending on its operating conditions. Several studies have investigated the flow patterns inside the cylinder and the effects of increasing swirl on engine performance. Researchers have also studied the behavior of the piston crown and its influence on turbulent flow and viscous disturbances. Various studies have focused on the development and growth of cracks in the engine cylinder and their effects.

One study specifically examined the failure analysis of a heavy-duty diesel engine, highlighting that increased combustion temperatures can lead to increased cylinder stress and potential engine failure. Another study involved analyzing and modeling the three-dimensional behavior of the engine piston to study stresses, strains, and the risk of fatigue failure.

These studies, as mentioned, examined the mechanical and thermal stresses generated during combustion and their effects on engine components. Such investigations are essential in designing more efficient and durable engines, optimizing their performance, and ensuring their reliability. Researchers used finite element

analysis and computational tools to understand and optimize engine components, especially in critical areas. They analyzed the impact of different conditions and loads, including torsional and bending forces, and calculated von Mises stress with theoretical foundations and computational software to provide insights for engine improvement and design.

Wanli and Yan [2] conducted a thermal simulation of the piston using a three-dimensional finite element method, considering one-dimensional heat resistance in the oil film. In another study, Harry Gaya and Toda [3] investigated the effect of flame speed on thermal flux in the combustion chamber. They calculated gas temperatures using a two-zone method and determined thermal flux at various points within the combustion chamber using an experimental approach. The results showed that an increase in flame speed led to a decrease in maximum thermal flux. In one of the most recent studies, Gots and Klevtsov [4] examined the reasons for the formation of cracks on the edges of the piston's combustion chamber. Generally, piston failures can result from mechanical and thermal loading, with thermal loads often contributing significantly to equivalent stresses. Therefore, cracks form gradually due to thermal loading, often leading to piston damage. Zhaoju and colleagues [5] calculated the distribution of piston temperature fields in a statically compressed state and the thermal-mechanical connection stresses, emphasizing that mechanical loads are the primary sources of principal stresses. Singh and Yadav [6], in a review study, focused on analyzing the piston design under thermal loads using a reference stress method.

In their research, Ramasamy et al.[7] explored the impact of thermal barrier coatings on engine efficiency and emissions. They applied yttria-stabilized zirconia (YSZ) and aluminum silicate ($Al_2O_3 \cdot SiO_2$) coatings to piston alloys using plasma spray. The study revealed that the YSZ coating enhanced engine performance, increasing brake thermal efficiency (BTE) to 15.94% for diesel and 14.55% for biodiesel, and reducing brake-specific fuel consumption (BSFC) to 498.96 g/kWh for diesel and 619.81 g/kWh for biodiesel. Conversely, ($Al_2O_3 \cdot SiO_2$) coatings were more effective in reducing emissions, showing lower levels of NO, CO, and CO2 for both fuel types. Uncoated pistons delivered higher torque and ignition, particularly with diesel, due to their higher viscosity and lower calorific value, and exhibited the lowest hydrocarbon emissions, suggesting complete fuel combustion. The findings indicate that YSZ coatings are preferable for engine performance, while ($Al_2O_3 \cdot SiO_2$) coatings are beneficial for reducing greenhouse gas emissions.

Margot et al.[8] discuss the automotive industry's shift towards using novel insulating materials with low thermal conductivity $< 0.4\ W/mK$ and heat capacitance $< 500\ kJ/m\text{^}3K$) to coat engine combustion chambers and exhaust manifolds. The goal is to reduce the thermal swing between the gas and walls during the engine cycle, thereby minimizing heat loss. Due to the challenges in measuring wall temperature, simulations are often employed. However, the thinness of the new coating layers ($\sim 100\mu m$) complicates numerical modeling, necessitating a novel approach. This paper introduces a strategy to simulate thin coatings by defining an equivalent thicker material that mimics the real coating's thermal behavior. Using 3D-CFD software, the study compares the performance of a conventional metallic piston and a coated piston top, highlighting the impact of these insulating coatings on engine efficiency.

Gangula et al.[9] investigated the effects of thermal barrier coatings (TBC) on CI engine pistons using diesel and mahua biodiesel (MB 100) as fuels. The study utilized three pistons with TBCs, consisting of a 0.05 mm bond coat and a 0.25 mm topcoat. The coatings varied: 7% YSZ (LHR 1), 2%Nd+YSZ (LHR 2), and 5%Nd+YSZ (LHR 3), with Ni-Cr-Al-Y as the bond coat for all. The research, conducted on a four-stroke, single-cylinder diesel engine, compared the standard engine's performance with diesel and mahua biodiesel against the three TBC pistons. Results indicated that the LHR 3 piston with mahua biodiesel improved brake thermal efficiency by 11% and reduced brake-specific fuel consumption by 13% compared to the standard engine. Additionally, HC and CO emissions decreased by 13% and 16%, respectively, while NOx emissions slightly increased by 18% for the LHR 3 engine.

In the study by Reddy et al.[10], the effects of thermal barrier coatings (TBC) on diesel engine pistons were examined. The pistons

were coated with three TBC materials: 7% YSZ, 2% (Gd_2O_3+YSZ), and 5% (Gd_2O_3+YSZ), each with a 0.25 mm thickness, over a 0.05 mm NiCrAlY bond coat. The plasma spray technique was used for deposition. Testing under various load conditions in a four-stroke single-cylinder diesel engine showed that TBCs increased brake thermal efficiency by 12.1% and decreased brake-specific fuel consumption by up to 16.2% compared to the baseline engine. Additionally, HC and CO emissions were reduced by 17.8% and 18.4%, respectively, while NOx emissions increased by 14.87%.

Balaji et al.[11] examine the influence of ceramic coatings on diesel engine performance, particularly when using biofuel from jatropha seed oil and methyl ester blends. The study suggests coating pistons with Cr_3C_2-PS. ZrO_2 powders to enhance thermal and wear resistance. Testing was conducted on a four-stroke single-cylinder diesel engine under varying loads, assessing combustion characteristics like heat escape, peak strain, ignition delay, and thermal brake performance. The results showed that pistons coated with the proposed materials increased engine performance by approximately 10% and cylinder pressure by 20% with Jatropha Methyl Ester (JME), compared to uncoated pistons. This indicates a significant improvement in wear resistance, with a 47% shift and an overall wear rate reduction of 35%.

In the study by Gehlot and Tripathi [12], the steady-state thermal analysis of a diesel engine piston with a ceramic coating featuring holes was conducted. The temperature distribution on both the piston's top surface and the substrate was analyzed using Ansys, a finite element-based software. The piston crown was coated with yttria-stabilized zirconia on an Al-Si alloy, with a ceramic top coating thickness of (0.4 mm) and a NiCrAl bond coat of (0.1 mm). The analysis varied the radius of the holes on the coating surface ((1.5 mm), (2 mm), and (2.5 mm)), finding that the top surface temperature increased with the hole radius, peaking at (2.5 mm). This contrasts with coatings without holes, where a significant rise in the piston's top surface temperature was noted. Conversely, the substrate temperature decreased as the hole radius increased.

Liu et al.[13] conducted a theoretical study on the thermo-mechanical conditions within a diesel engine piston. They utilized operational parameters, semi-empirical formulas, and empirical models to establish boundary conditions like temperature and stress fields. The finite element method (FEM) was applied to calculate stress loading and fatigue life. The empirical formulas and models were refined using experimental data and verified through accelerated life testing. The study found that piston life and stress relationships under various loads conform to the Arrhenius model, Inverse ignition law model, and Generalized Eyring model, depending on the type of load condition.

Lu et al.[14] present a novel calculation method for designing pistons in high-performance diesel engines to withstand increased thermal loads. They developed a 3D solid model of a piston for a 16V280 diesel engine and conducted simulations to analyze steady-state and transient-state temperature fields. The study found that the maximum temperature fluctuation in the piston temperature field was less than 20 degrees Celsius, allowing the steady-state temperature field to be used as a boundary condition for thermal stress calculations. The thermal mechanical decoupling method indicated that the maximum temperature reached 354°C at the combustion chamber's edge, and the maximum thermal stress was 270MPa, which is within the permissible range. The most critical area identified was at the combustion chamber throat and the piston head and skirt contact area. This research contributes to the optimization of piston design by providing a theoretical foundation for managing thermal stress.

Vedharaj et al.[15] investigated the use of CNSL (cashew nut shell liquid) for biodiesel production and its effects on diesel engine performance with and without a coating. The study utilized PSZ (partially stabilized zirconia) as a coating material for engine pistons, valves, and cylinder heads. The findings from the experimental and simulation studies using FEA (finite element analysis) showed that CNSL biodiesel (25% CNSLME and 75% diesel) in a coated engine increased brake thermal efficiency (BTE) by 6%. Additionally, emissions of CO, HC, and smoke were reduced by 27.7%, 7.2%, and 14.3%, respectively, while NO_x emissions increased. The thermal stress analysis confirmed that the

coated piston had lower average temperature, heat flux, and thermal stress, leading to improved thermal efficiency.

Buyukkaya and Cerit[16] conducted thermal analyses on conventional diesel pistons made of aluminum silicon alloy and steel, as well as pistons coated with $MgO - ZrO_2$. Using ANSYS software, they compared the results of four different pistons to assess the impact of coatings on their thermal behavior. The study found that coating pistons with materials of low thermal conductivity significantly improved the maximum surface temperature by about 48% for the AlSi alloy and 35% for the steel.

Witeka and Zelek's[17] study delves into the failure and stress analysis of a connecting rod in a turbocharged diesel engine. They employed finite element method (FEM) for an advanced stress analysis, creating geometrical models of the connecting rod and related components. The analysis under maximum engine ignition revealed high-stress zones at the crack origins, influenced significantly by the bolt-tightening torque. The findings suggest that the primary cause of the connecting rod's failure was high stress near the bolt hole, exacerbated by high bolt pretension and a small fillet radius, leading to a notch effect and additional stress concentration. The study concludes with recommendations to enhance the fatigue life of the connecting rod.

A comprehensive overview of the engineering literature suggests that the individual analysis and examination of each diesel engine component still plays a vital role in their design and performance. As mentioned, most research primarily focuses on the simultaneous analysis of one or two components. The extraction of design knowledge and methods for enhancing the thermal performance of a marine diesel engine's components are areas that remain relatively unexplored. The remarkable innovation in this research involves not only the mechanical analysis of fundamental components for ignition generation but also the presentation of solutions to reduce thermal stresses and improve performance in Mercury Marine diesel engines.

3. Research Method

3.1. Engine Dimensions and Measurements

To perform numerical analysis based on the finite element method and evaluate the results, we first create a model of the Mercury Marine diesel engine by its real dimensions and existing technical drawings. These dimensions and measurements are provided in millimeters, as shown in Figs. (1) to (4)

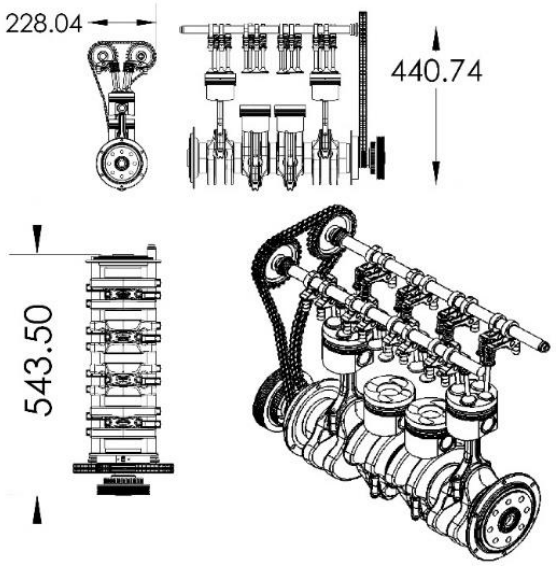

Fig. 1. Three views and provided dimensions for the assembled CAD Model of the Mercury Marine engine, model L4 Tier 3 with an ignition of 150 horse-ignition

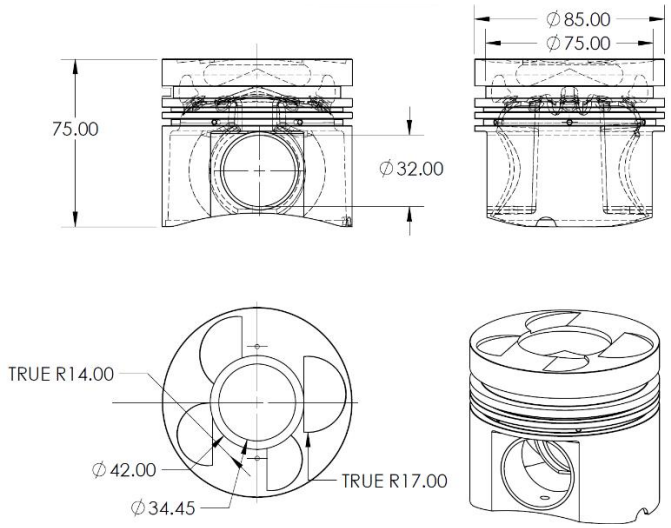

Fig. 2. Three views and provided dimensions for the piston.

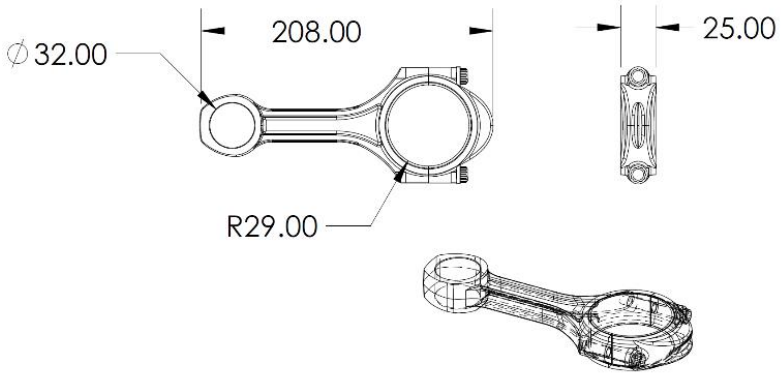

Fig. 3. Three views and provided dimensions for the connecting rod.

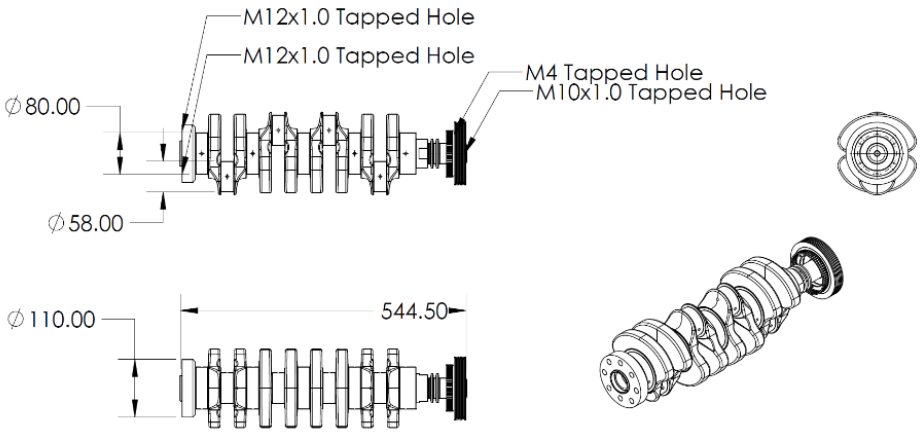

Fig. 4. Three views and provided dimensions for the CrankShaft.

Due to the excessive complexity of Mercury engine components, the main drawings are simplified to improve the quality of numerical modeling and reduce the time and cost of finite element analysis. Therefore, the drawings related to Figs. (5) to (8) are used for modeling the components by SolidWorks software.

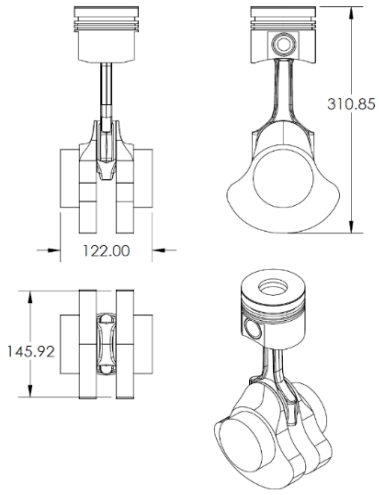

Fig. 5. Simplified three views and dimensions for the assembled CAD Model of the Mercury Marine engine, model L4 Tier 3 with 150 horse-ignition

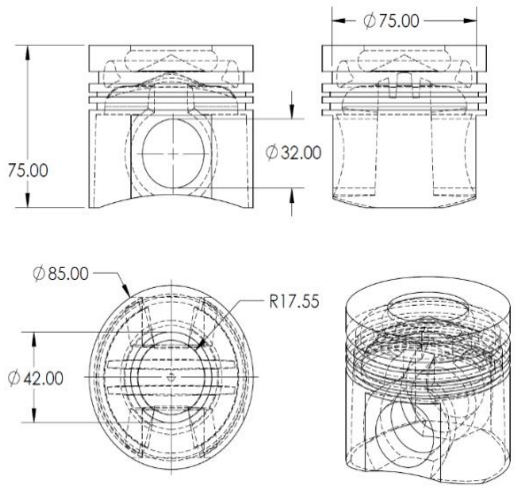

Fig. 6. Three views and dimensions for the simplified piston model.

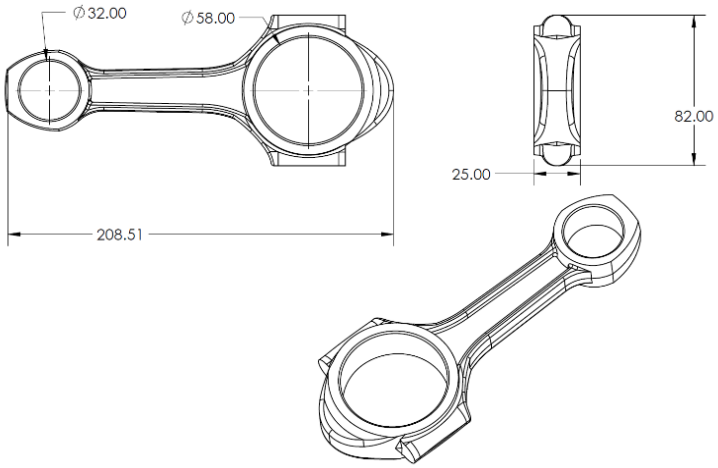

Fig. 7. views and dimensions for the simplified connecting rod model.

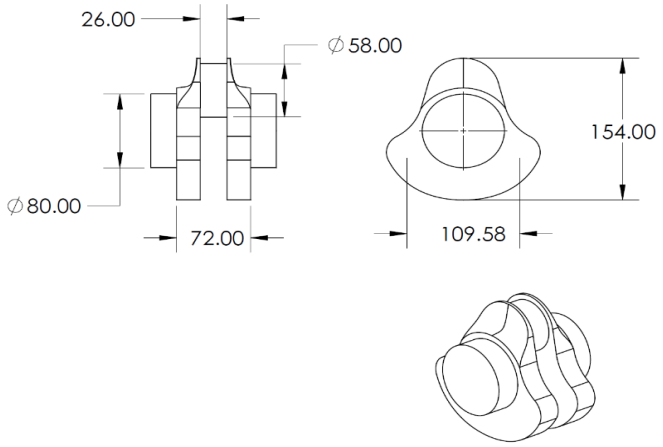

Fig. 8. Three views and dimensions for the simplified crankshaft model.

The Mercury diesel engine is a four-cylinder, inline engine, and due to the arrangement of the pistons, the shape of the CrankShaft is symmetrical. Therefore, to reduce the analysis time and because the focus of this research is mainly on the piston and the thermal and mechanical loads applied to it, only a part of the CrankShaft, as shown in Fig. 8, is used in the numerical modeling.

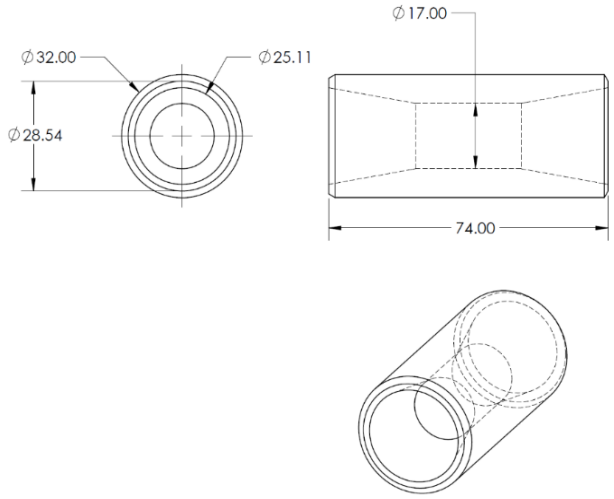

Fig. 9. Three views and simplified dimensions for the engine's Gudgeon pin.

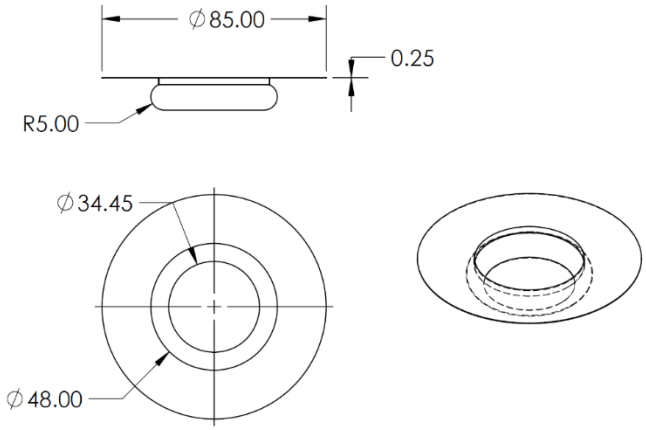

Fig. 10. Three views and designed dimensions for the piston head coating by ceramic.

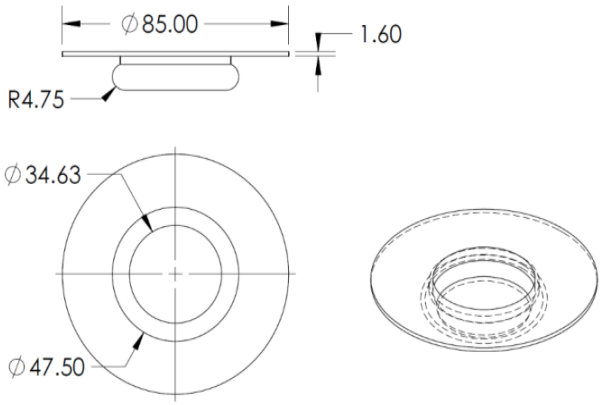

Fig. 11. Three views and designed dimensions for Communication coverage to coating the piston.

3.2. Material Selection

After designing and three-dimensional modeling of the engine components using SolidWorks, Abaqus software is used for numerical modeling. Accurate modeling requires having the specifications and characteristics of the materials used in the construction of diesel engine parts.

The piston's function and the loads applied to it impose specific requirements on the material of the piston. If a lightweight piston is desired, materials with lower density are preferred. In addition to the design shape, the material's strength is a determining factor for the piston's load-carrying capacity. Load changes over time require good static and dynamic resistance. Thermal resistance is also crucial due to thermal loads.

Given the reciprocating motion of the piston, choosing the right material to reduce friction and wear between the piston and the cylinder wall is essential in piston design. Considering the high temperature in the cylinder chamber, taking the thermal conductivity of the piston material into account can help improve heat dissipation, reduce piston temperature, and prevent damage caused by thermal stresses.

Considering the requirements for piston material, the recommended material for the piston is the aluminum alloy M124P, whose mechanical properties are listed in Table (1) [18].

Table 1. Physical and Mechanical Properties of the Recommended Material for Mercury Engine Piston

Features		**M124P**
HB10 Harness	20°C	100-125
Tensile strength R_m [MPa]	20°C	100-125
	150°C	250-300
	250°C	80-140
	300°C	50-100
Yield point $R_{P0.2}$ [MPa]	20°C	280-340
	150°C	220-280
	250°C	60-120
	300°C	30-70
Fracture elongation A_5 [%]	20°C	1<
	150°C	4
	250°C	20
	300°C	30
Fatigue strength under reverse bending stress formula σ_{bw} [Mpa]	20°C	110-140
	150°C	90-120
	250°C	45-55
	300°C	30-40
Young's modulus [MPa]	20°C	80000
	150°C	77000
	250°C	72000
	300°C	69000
Thermal conductivity [W/mk°] λ	20°C	155
	300°C	165
Thermal expansion $\alpha[10^{-6}\mathrm{m/mK}]$	20-100°C	19.6
	20-200°C	20.6
	20-300°C	21.4
Density $\rho[\frac{g}{cm^3}]$	20°C	2.68

Diesel engines endure higher pressure and forces compared to gasoline engines. Therefore, the connecting rod must be made of a strong and sufficiently robust material to withstand the demanding conditions of diesel engine operation. The connecting rod must be constructed from materials that can withstand material fatigue and cyclical stresses from the engine. Selecting the appropriate material and following suitable manufacturing processes can enhance the strength and durability of the connecting rod.

The piston pin in diesel engines is subject to high torque and substantial pressures. Hence, the material must have adequate resistance against these forces. The performance of the piston pin is closely related to wear and friction. The material for the piston pin should possess characteristics that not only guarantee a long service life but also enable suitable machinability for the manufacturing processes of the piston pin. For this reason, the connecting rod and piston pin in the Mercury engine are made from heat-treated 42CrMo4 chrome-molybdenum alloy steel. The physical and mechanical properties of the proposed material 42CrMo4, temperature-dependent, are provided in Table (2) [19].

Table 2. Physical and Mechanical Properties of the Proposed Material for the Connecting Rod and Piston Pin in the Mercury Engine

Features	42CrMo4	
Tensile strength R_m [MPa]	20℃	920-980
	130℃	870-960
	300℃	850-930
	450℃	630-690
Yield point $R_{P0.2}$ [MPa]	20℃	740-860
	130℃	700-800
	300℃	680-750
	450℃	530-580
Fracture elongation A_5 [%]	20℃	12-15
	130℃	8-13
	3000℃	10-13
	450℃	15-16
Fatigue strength under reverse bending stress formula σ_{bw} [Mpa]	20℃	370-440
	130℃	350-410
	300℃	340-400
	450℃	280-340
Young's modulus [MPa]	20℃	212000
	130℃	203000
	300℃	193000
	450℃	180000
Thermal conductivity λ [W/mk^o]	20℃	44
	130℃	43
	300℃	40
	450℃	37
Thermal expansion $\alpha[10^{-6}\mathrm{m/mK}]$	20-300℃	13.2
	20-450℃	13.7
Density $\rho[\frac{g}{cm^3}]$	20℃	2.68

3.2.1. Piston Crown Coating Process

Piston crown coating is a production process in which a layer of material is applied to the piston head surface to enhance its performance, resistance, and durability. This process is mainly carried out to improve resistance to heat, pressure, wear, and corrosion, and extend the useful life of the piston crown. The main phases of piston crown coating include surface preparation, coating, drying, curing, and machining and correction. This process is typically performed using specialized technologies such as electrolytic coating, plasma coating, powder coating, etc. The primary goal of piston crown coating is to improve the properties of the piston crown and increase its useful life under various engine operating conditions.

The use of a bond coat material in piston crown coating serves important purposes such as optimizing heat transfer, absorbing pressure and deformation, protecting surfaces, reducing noise and vibration, and facilitating machining and installation. In general, the use of a bond coat material in piston crown coating is carried out to enhance performance, protect components, reduce undesirable effects, and extend the useful life of the piston crown. On the other hand, to select a suitable material for the main coating in piston crown coating (covering with layers of materials on the piston head of engines), characteristics such as resistance to heat, pressure, wear, corrosion, thermal properties, and cost should be taken into account. Therefore, the proposed material for piston crown coating includes NiCrAl alloy for the bond coat material and La2Ce2o7 ceramic for the coating material. The physical and mechanical properties related to these two proposed materials are provided in Table (3) [20].

Gudgeon pin, due to its endurance of recurring and cyclic loads, imposes a set of requirements for material selection. The material for the gudgeon pin needs to have not only suitable mechanical strength but also high resistance to wear and corrosion. Its tolerance to thermal loads, given its contact with the piston, is of particular importance.

Therefore, a heat-treated 16MnCr5 alloy is used for the gudgeon pin material. The physical and mechanical properties related to this recommended material are provided in Table (4) [21].

3.2.2. Finite Element Modeling

The three-dimensional models of the components have been designed using SolidWorks software, conforming to the real and existing dimensions of the Mercury diesel engine.

Table 3. Physical and Mechanical Properties of the Proposed Material for Piston Crown Coating in Mercury Engine

Material	Density $[kg/m^3]$	Specific heat $[J/kg°C]$	Thermal diffusivity $[10^{-6}(\frac{1}{°C})]$	Thermal conductivity $[W/m°C]$	Young's modulus [GPa]	Poisson's ratio $[m/m]$
(NiCrAl)	787	764	12	16.1	90	0.27
($La_2Ce_2o_7$)	6290	430	12.3	0.6	25	0.29

Table 4. Physical and Mechanical Properties of the Proposed Material for Gudgeon Pin in Mercury Engine

Material	Tension strength R_m [MPa]	Yield point $R_{P0.2}$ [MPa]	Fracture elongation A_5 [%]	Thermal expansion $\alpha\left[\frac{10^{-6}m}{mK}\right]$	Thermal conductivity λ[W/mK]	Density $\rho[\frac{g}{cm^3}]$	Poisson's ratio $[m/m]$	Young's modulus [GPa]
Alloy 16MnCr5	880-1230	600	10	16.2	52	7850	0.29	200

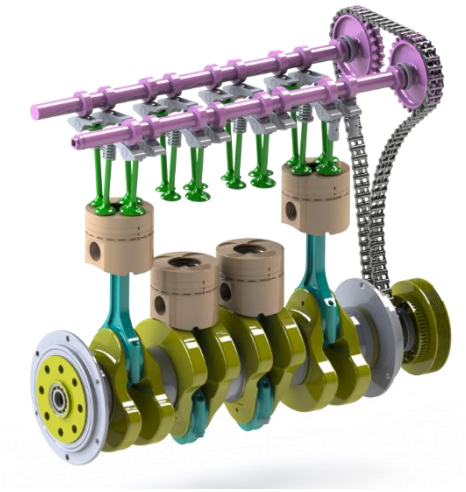

Fig. 12. Three-Dimensional Model of the Real Assembly of the Mercury Engine Components

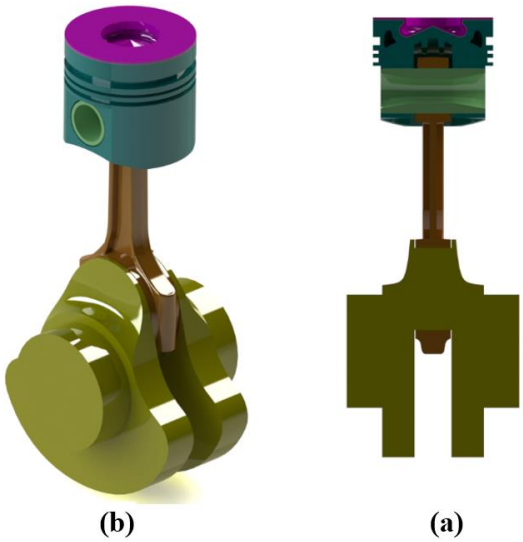

Fig. 13. Three-Dimensional Model of the Simplified Assembly of the Mercury Engine Components – (a) 3D View – (b) Cross-sectional View

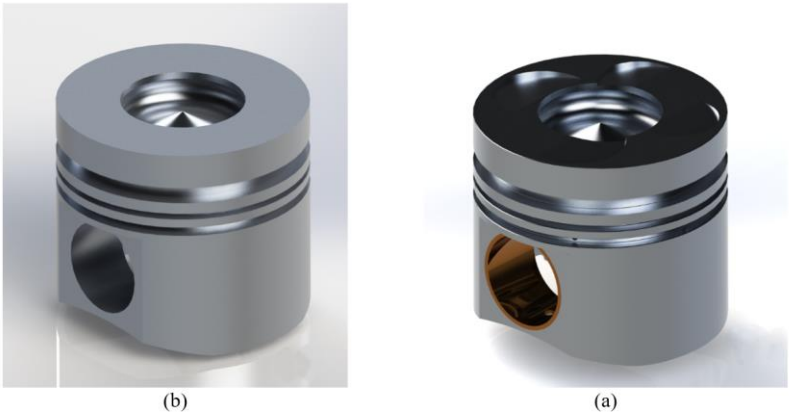

Fig. 14. Three-Dimensional Modified Model for the Piston – (a) Model without Changes – (b) Simplified Model

(b) (a)

Fig. 15. Three-Dimensional Modified Model for the Connecting Rod – (a) Model without Changes – (b) Simplified Model

(b) (a)

Fig. 16. Three-Dimensional Modified Model for the CrankShaft – (a) Model without Changes – (b) Simplified Model

Fig. 17. Three-Dimensional Modified Model for the Gudgeon pin.

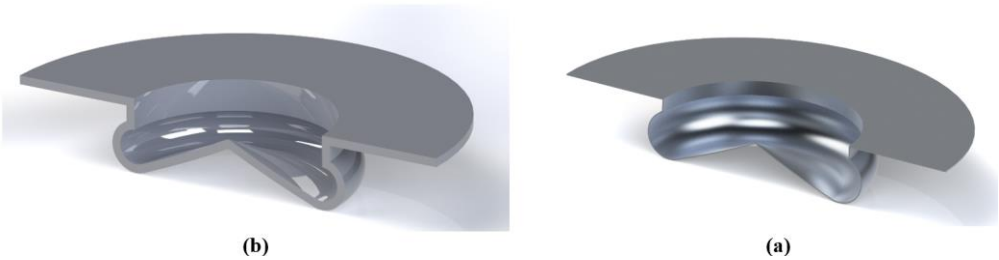

(b) (a)

Fig. 18. Three-Dimensional Modified Model for the Interface Coating, (b) Three-Dimensional Modified Model for the ceramic Coating.

Figure 19 to Fig. 24 illustrate the meshing of components of the Mercury Marine engine for numerical modeling and result evaluation. The information related to the material and substances of the components (including the piston, connecting rod, crankshaft, Gudgeon pin, quenching interface coating, and main quenching coating), boundary conditions, and equations governing the problem, along with the assembled three-dimensional model, is utilized by Abaqus software for numerical modeling.

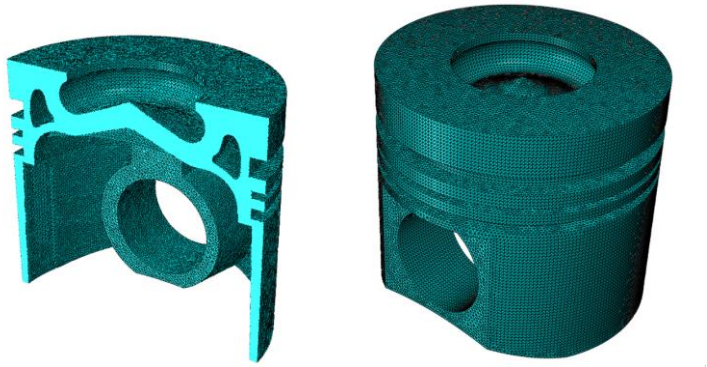

Fig. 19. Finite element model with meshing of the piston and a section view

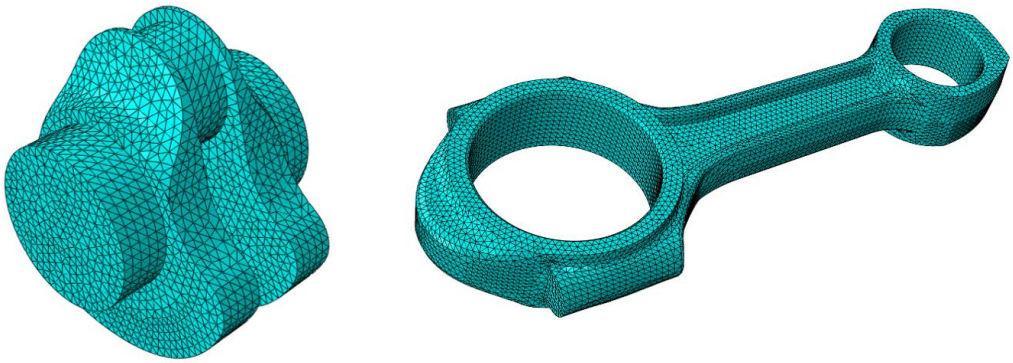

(b) **(a)**

Fig. 20. (a) Finite element model with meshing of the connecting rod, (b) Finite element model with meshing of the crankshaft

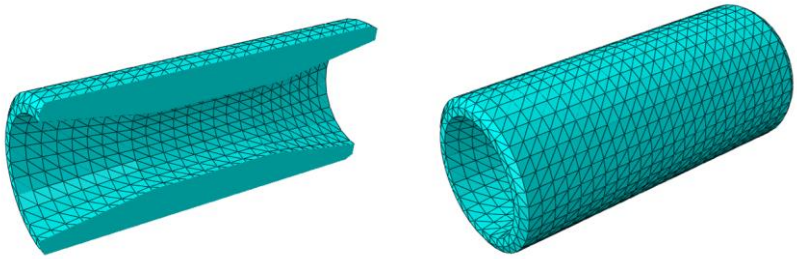

Fig. 21. Finite element model with meshing of the Gudgeon pin and a cutaway view

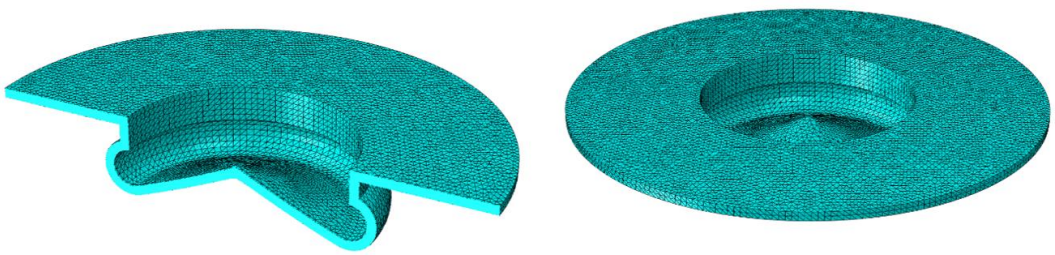

Fig. 22. Finite element model with meshing of the interface coating cover and a cutaway view

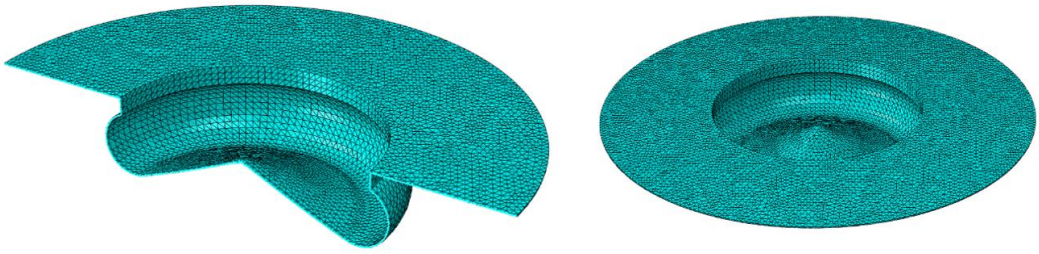

Fig. 23. Finite element model with meshing of the coating cover and a cutaway view

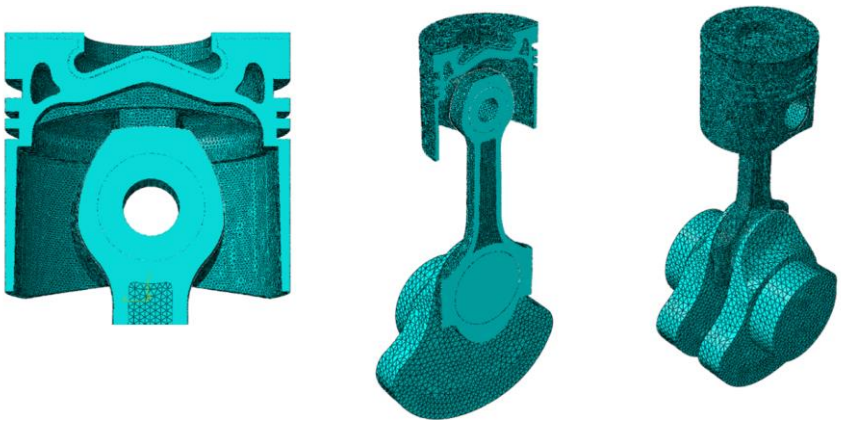

Fig. 24. Finite element model with meshing of the assembly model of the Mercury engine and a cutaway view

To ensure accurate analysis and achieve reliable results, the size of the mesh plays a fundamental role in the model. Therefore, a trial-and-error method has been employed to select the most suitable type of element and the optimal size for the elements. In this process, the numerical analysis is initially performed with a chosen type and size of the element. Subsequently, the size of the elements is modified, and another round of numerical analysis is conducted. By iteratively examining the convergence of results, the most appropriate element type and optimal size for the elements are determined. Table (5) displays the meshing information for components of the Mercury engine.

It is worth mentioning that, despite the need for ignitionful computer hardware systems and the time-consuming nature of the simulation process, the numerical analysis and simulation have been conducted implicitly and dynamically to achieve results close to real conditions. The innovation in this type of analysis lies in the ability to evaluate stress, and strain levels for any chosen element of the analyzed components at any angle of the crankshaft.

The flowchart that show the way to dynamical simulation of the diesel engine in ABAQUS is as below.

Table 5. Meshing information for components of the Mercury engine

Piece's name	Number of nodes	Minimum distance between knots [mm]	Element type	Number of elements
Piston	1075813	1	A linear tetrahedron of typeC3D4	211093
Connecting rod	94870	2		20268
Crankshaft	58710	5		11835
Gudgeon pin	11066	3		2654
Coating interface	50281	1		16936
The main coating	101063	1		25503

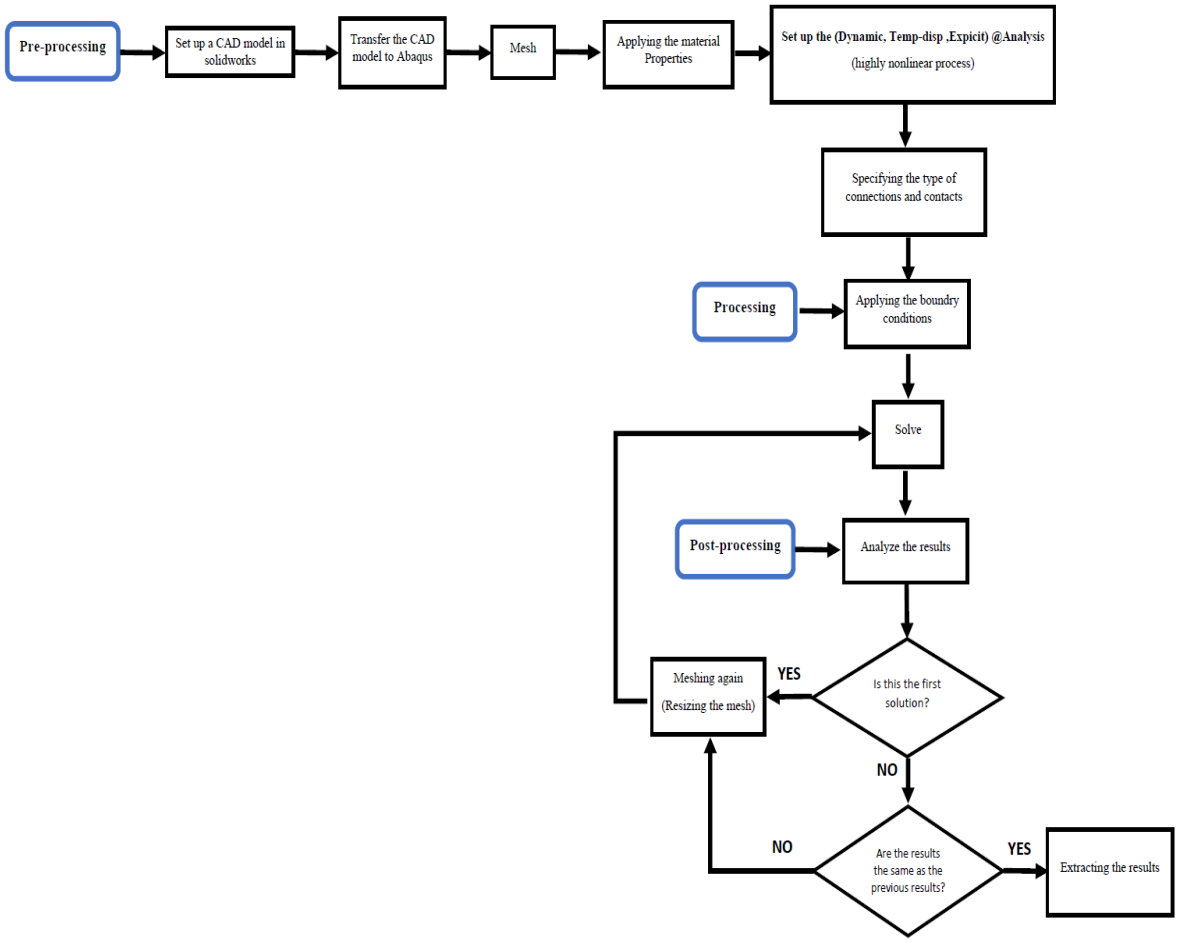

4. Data Analysis

4.1. Dual Cycle Analysis

Considering that this research focuses on the analysis of piston, connecting rod, and crankshaft components for a Mercury marine engine with a ignition of 150 horseignition, all equations governing the conditions of the problem have been coded and implemented using MATLAB programming language to extract and utilize the results in evaluating the specified engine. The assumptions for thermodynamic modeling of the Mercury engine using experimental data are presented in Tables (6) to (9).

Table 6. Geometric Information and Assumptions for Mercury Diesel Engine

Displaced volume in liters	$V = 2$
Number of engines cylinders	$N = 4$
Engine crankshaft rotation speed in RPM	$n = 2800$
Compression ratio	$r_c = 16$
Ratio of the piston displacement in one stroke to the piston diameter	$X = 1.24$
Mechanical efficiency	$\eta = 0.86$
Internal EGR percentage	* $EGR = 2$
Percentage of added heat during a constant volume process	$cvp = 20$
Percentage of added heat during a constant pressure process	$cpp = 100 - cvp$

*EGR (Exhaust Gas Recirculation) percentage measures the amount of exhaust gases that are being recirculated in the combustion chamber of the engine. This criterion is commonly used in diesel engines as a means to reduce NOx emissions. The EGR percentage is the ratio of the mass of recirculated exhaust gases to the mass of fresh air entering the engine, expressed as a percentage. A higher EGR percentage means that more exhaust gases are in the process of recirculation, which can have both positive and negative effects on engine performance and emissions

Table 7. Fuel Information and Combustion Efficiency

The number of Carbon atoms	$x = 12$
The number of Hydrogen atoms	$y = 23$
Air to Fuel mass ratio	$AF = 18$
Combustion efficiency	$\eta_{conv} = 1$

Table 8. Working Fluid Properties for Mercury Engine

Specific heat ratio of Air	$k = 1.35$
Particular Gas Constant of Air	$R = 0.287 \frac{kJ}{kg.K}$
Specific heat for constant volume of air	$c_v = 0.821 \frac{kJ}{kg}$
Specific heat for constant pressure of air	$c_p = R + c_v$

Table 9. Atmospheric Properties for Mercury Engine

Atmospheric pressure	$P_0 = 100\,kPa$
Combustion chamber temperature at the start of compression	$T_0 = 60°C$
Air density in reference condition	$\rho_0 = \frac{P_0}{293.15\,R} \frac{kg}{m^3}$

One of the essential aspects in the analysis and calculation of stress, and strain values in the engine mechanism, which plays a key role in accurate calculation and modeling, is the P-θ and T-θ diagrams for the engine. Dual-cycle equations were used for obtaining these diagrams in the Mercury engine thermodynamic modeling.

Figure (25) to (27) shows the pressure-crank angle, pressure-volume, and temperature-crank angle diagrams for the Mercury engine at each moment, utilizing the written codes.

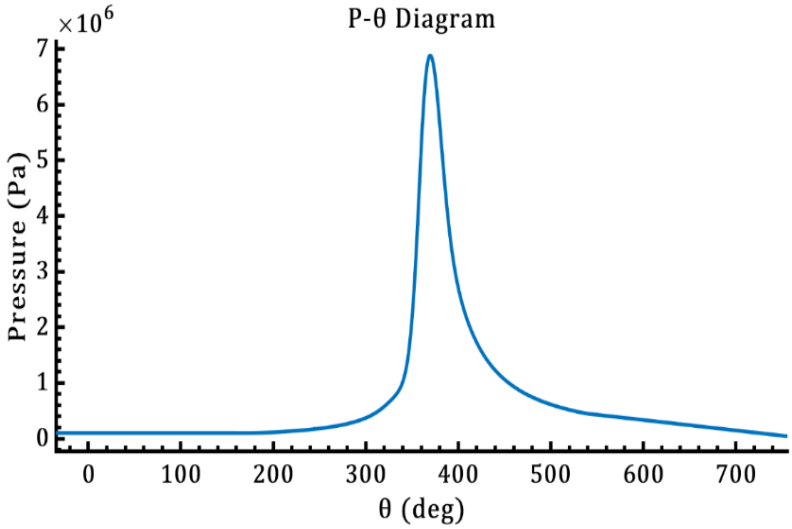

Fig. 25. P-θ diagram (piston pressure versus crank angle) for the Mercury engine based on the dual cycle obtained from the MATLAB code

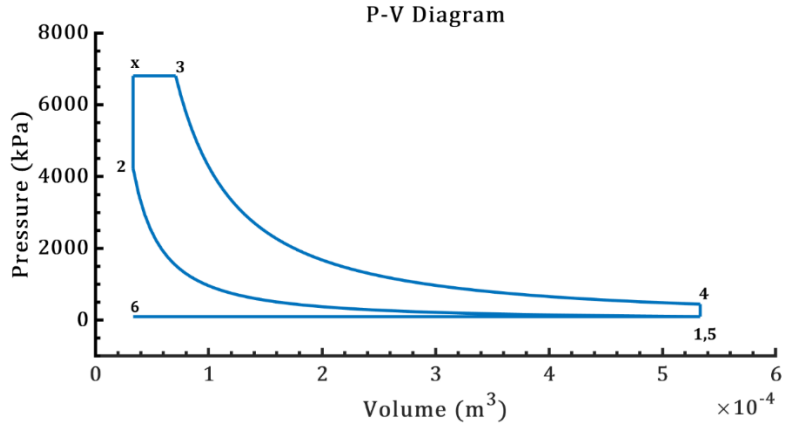

Fig. 26. P-V diagram for the Mercury engine based on the dual cycle obtained from the MATLAB code

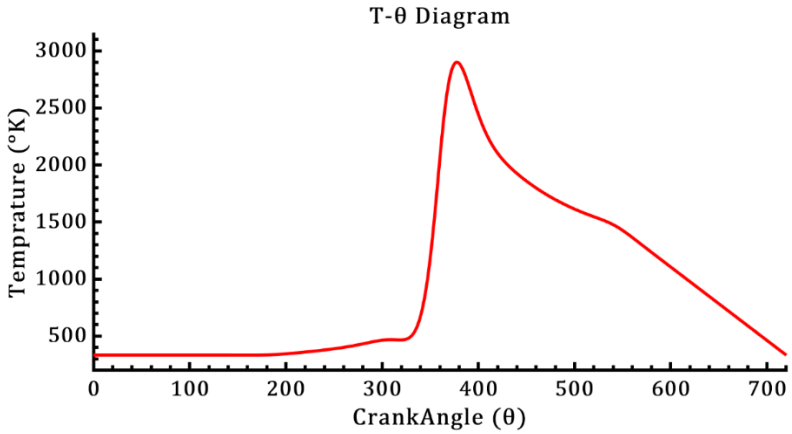

Fig. 27. T-θ diagram (combustion chamber temperature versus crank angle) for the Mercury engine based on the dual cycle equations obtained from the MATLAB code.

In the diagram in Fig. (26), the origin represents the measurement of crank angle changes, the bottom dead center (BDC) point, and the moment of the start of the compression process. Figure (28) and (29) show pressure-crank angle and pressure-volume diagrams at each moment for the Mercury engine using experimental data. Based on these diagrams, the maximum pressure and temperature in the dual cycle for the Mercury engine are obtained as 68 bar and 2700 degrees Celsius, respectively.

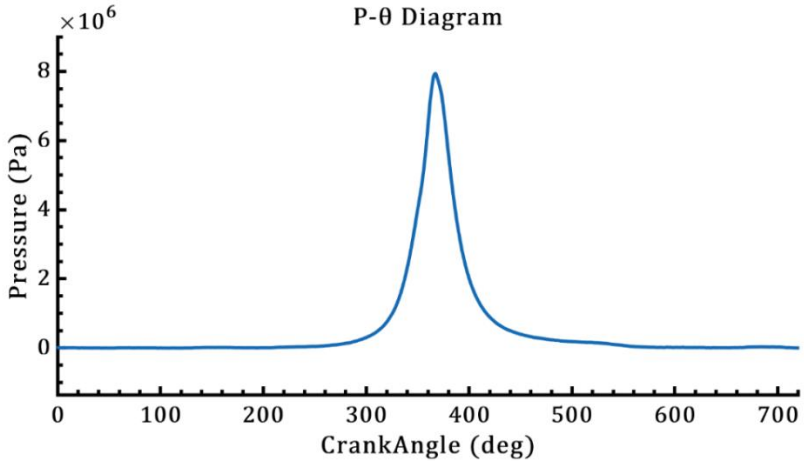

Fig. 28. Pressure-Crank Angle (P-θ) diagram for the Mercury engine based on measured data from the cylinder chamber.

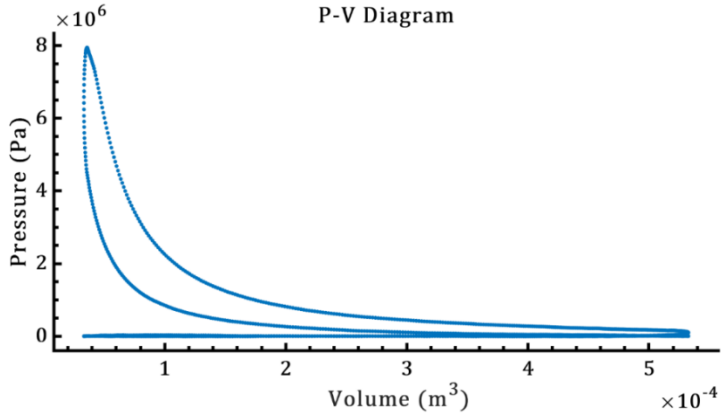

Fig. 29. Pressure-Volume (P-V) diagram for the Mercury engine based on measured data from the cylinder chamber

Given the diagrams in Fig. (30) and (31), the dual cycle, due to the addition of two constant-volume and constant-pressure processes to the standard diesel cycle, is closer to the real diesel cycle. Therefore, for numerical analysis in Abaqus, the results obtained from the written codes for the dual cycle have been used. Table (10) is used for boundary conditions, which is the result of running the MATLAB code.

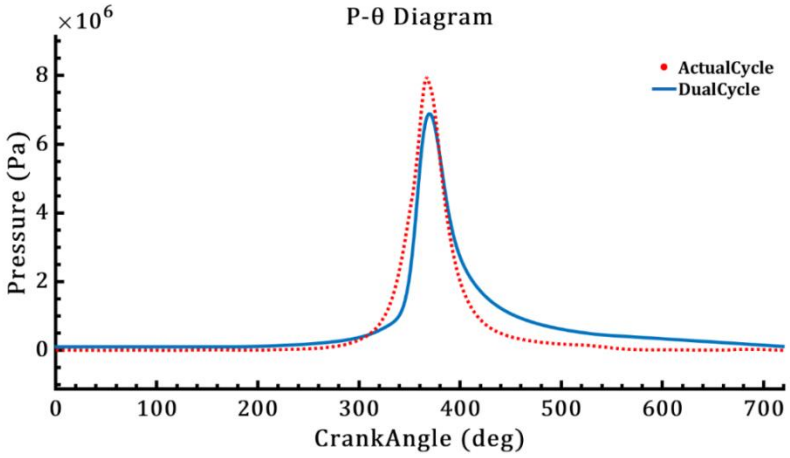

Fig. 30. Comparative diagram of P-θ (pressure-crank angle) for the Mercury engine based on measured data from the cylinder chamber and the dual cycle.

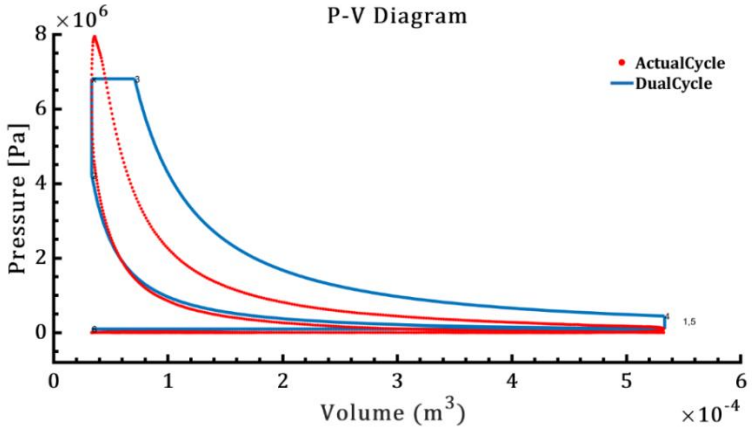

Fig. 31. Comparative diagram of P-V (pressure-volume) for the Mercury engine based on measured data from the cylinder chamber and the dual cycle.

Table 10. Results Obtained from Executing MATLAB Code for the Dual Cycle

Fuel and combustion properties	
Stochiometric air-fuel ratio	12.4649
Theorical air percentage	144.4055
Excess air percentage	44.4055
Fuel heating value	42788.3717kJ/kg
Characteristic of the operating point of cycle	
Maximum cycle temperature	2736.761°C
Maximum cycle pressure	6805.6419kPa
Overall engine performance	
Average piston speed	19.52m/s
Thermal efficiency	0.57
Average effective pressure	1407.7kPa
Engine ignition at2800 rpm	147hp
Frictional ignition lost	27hp
Torque at 2800 /min	192.7Nm
Special brake fuel consumption	171.18gr/kWh
Volume efficiency	0.87
Output ignition depending on displacement	70.24hp
Cutoff ratio	2.125

4.2. Investigating the Effect of Piston Bottom Temperature on the Mechanical Behavior of the Mercury Diesel Engine

To investigate the effect of temperature and thermal stresses on the components of the Mercury engine, including the piston, Gudgeon pin, connecting rod, and crankshaft, the first analysis did not consider the temperature of the piston bottom under boundary conditions. In the next step, the second analysis was performed by applying the temperature of the piston bottom under boundary conditions.

The numerical analysis was conducted for the Mercury engine at 2800 RPM. To prevent unreasonable increases in inertia forces, the rotational speed values of the connecting rod were applied with a function, reaching 293 radians per second (2800 RPM) from zero speed, under boundary conditions (Due to the prevention of excessive effects of inertial resistance forces on the results). Figure (32) shows the rotational speed of the connecting rod as a function of the crank angle. Figure (33) to (41) illustrate the contour plots of maximum piston stress, and strain without thermal effects for the four phases of intake, compression, ignition, and exhaust, which constitute one engine cycle with two revolutions of the crankshaft.

4.2.1. Dynamic Simulation of the Mercury Engine without Applying Thermal Effects

For the piston in the first analysis without thermal effects, in the intake phase, the maximum stress is 32 MPa. In the compression phase, the stress increases by 30% from the intake phase and reaches 47 MPa.

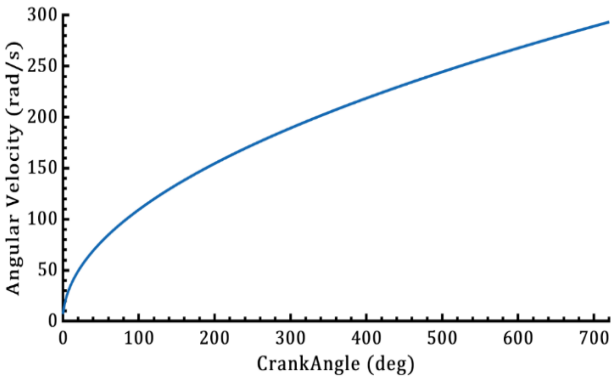

Fig. 32. rotational speed of the connecting rod as a function of the crank angle in the dynamical simulation

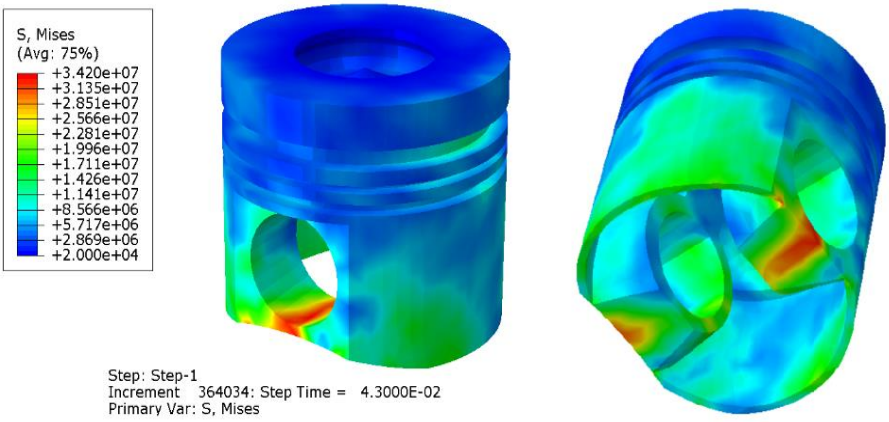

Fig. 33. Contour of maximum stress for the piston in the intake phase with applied pressure on the piston crown and without applying thermal effects

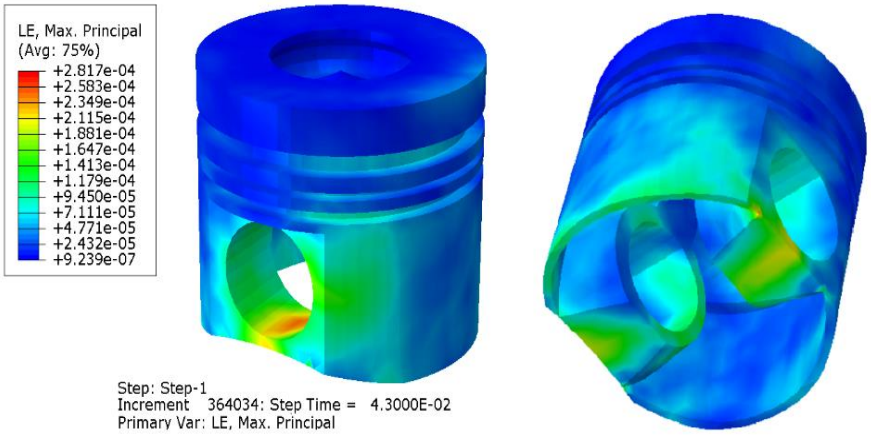

Fig. 34. Contour of maximum strain for the piston in the intake phase with applied pressure on the piston crown and without applying thermal effects

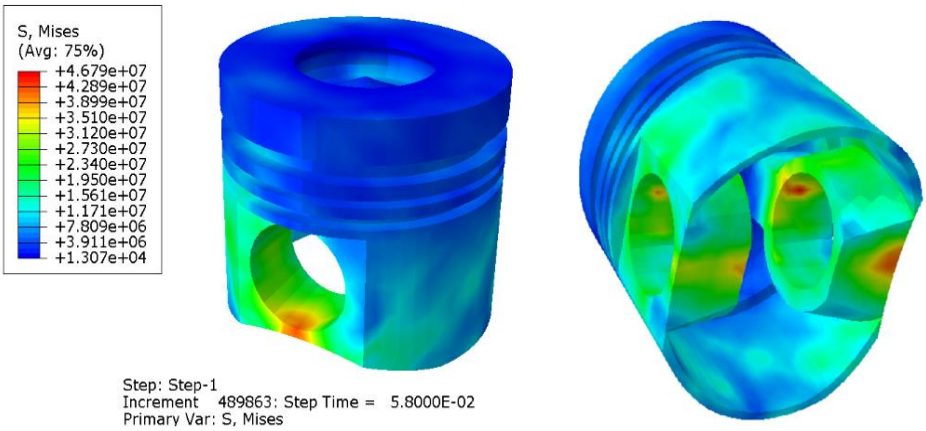

Fig. 35. Contour of maximum stress for the piston in the compression phase with applied pressure on the piston crown and without applying thermal effects

Based on Fig. (37), in the first analysis without thermal effects, the critical element of the piston located in the piston pinhole experiences a stress of 115 MPa during the ignition phase. This shows a noticeable increase compared to the maximum stress in the compression phase.

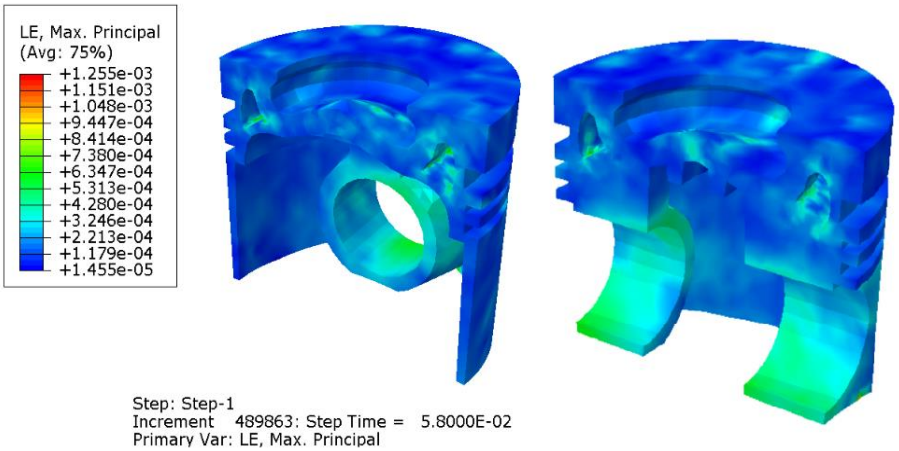

Fig. 36. Contour of maximum strain for the piston in the compression phase with applied pressure on the piston crown and without applying thermal effects

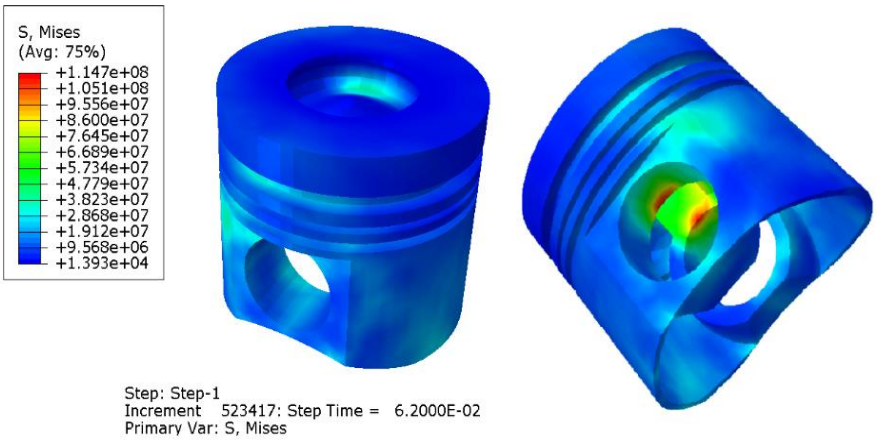

Fig. 37. Contour of maximum stress for the piston during the ignition phase with applied pressure on the piston crown and without the influence of thermal effects.

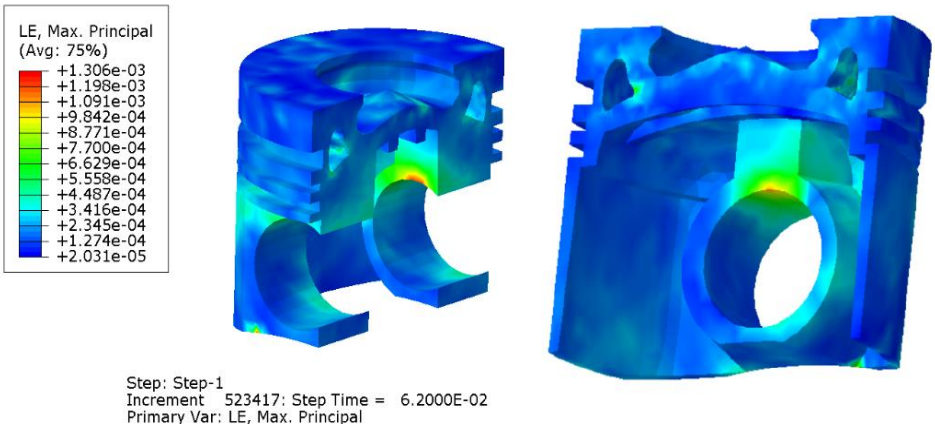

Fig. 38. Contour of maximum strain for the piston during the ignition phase with applied pressure on the piston crown and without the influence of thermal effects.

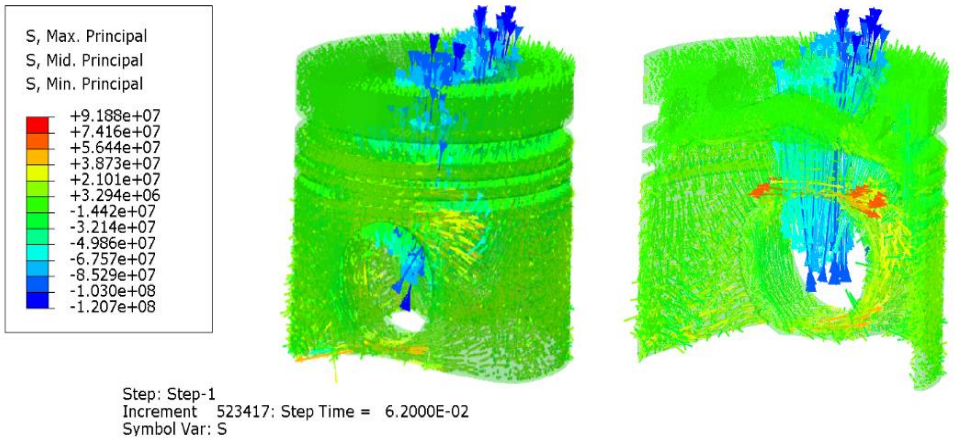

Fig. 39. Display of stress type (compressive or tensile) for the piston during the ignition phase with applied pressure on the piston crown and without the influence of thermal effects.

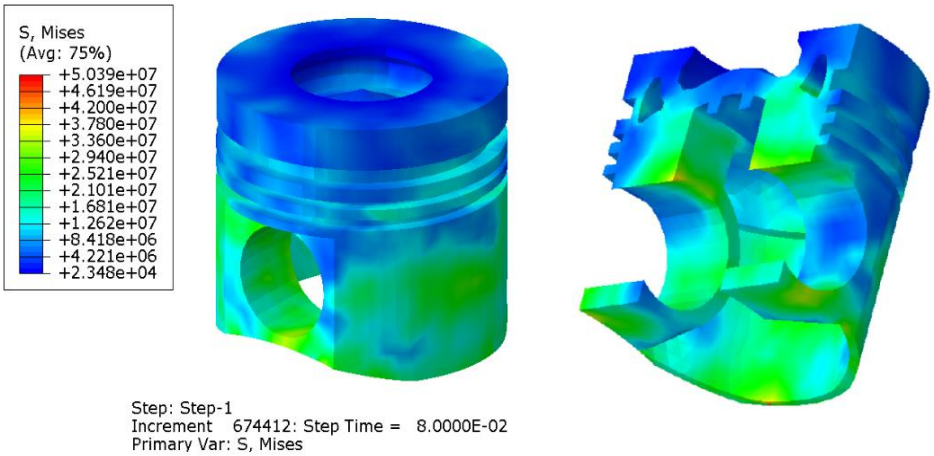

Fig. 40. Contour of maximum stress for the piston in the exhaust phase with applied pressure on the piston crown and without applying thermal effects.

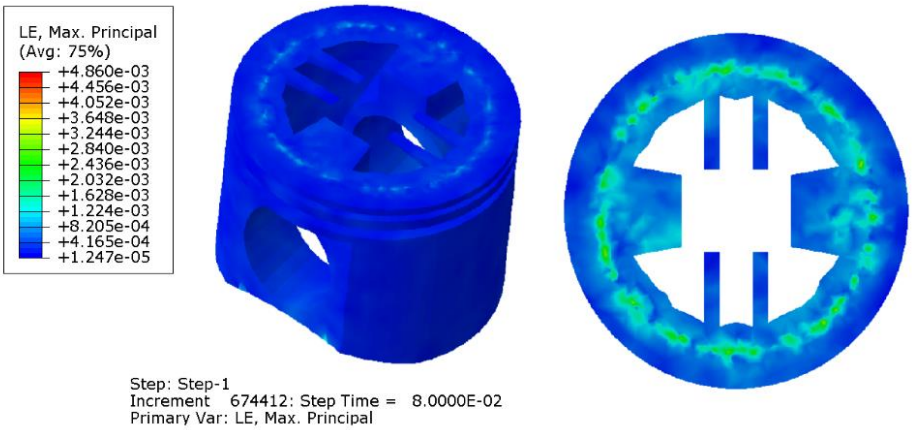

Fig. 41. Contour of maximum strain for the piston in the exhaust phase with applied pressure on the piston crown and without applying thermal effects.

In the exhaust phase, the maximum stress in the piston without thermal effects is 50 MPa. According to the results of the first analysis with applied pressure on the piston crown and without thermal effects at 2800 RPM, the maximum stress occurs in the ignition phase and the elements of the connection between the piston and the Gudgeon pin. Therefore, for a proper conclusion, stress, and strain diagrams versus crank angle have been extracted for the critical piston element in the ignition phase, as shown in Fig. (42) and (43).

Figure (44) to (49) depict the contour plots of maximum stress, and strain for the Gudgeon pin, connecting rod, and crankshaft in the ignition phase.

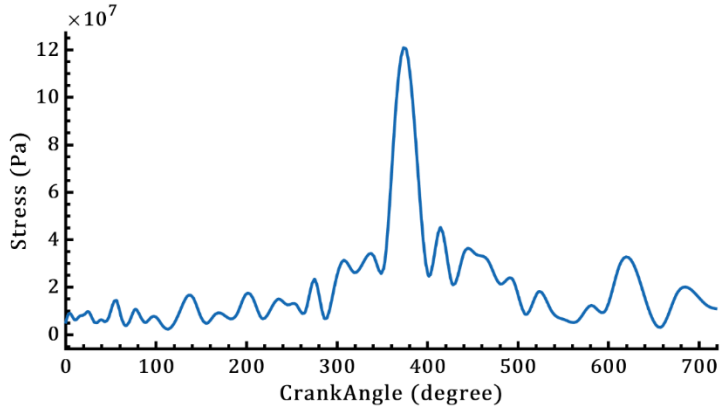

Fig. 42. Stress diagram versus crank angle for the critical piston element in the ignition phase without thermal effects.

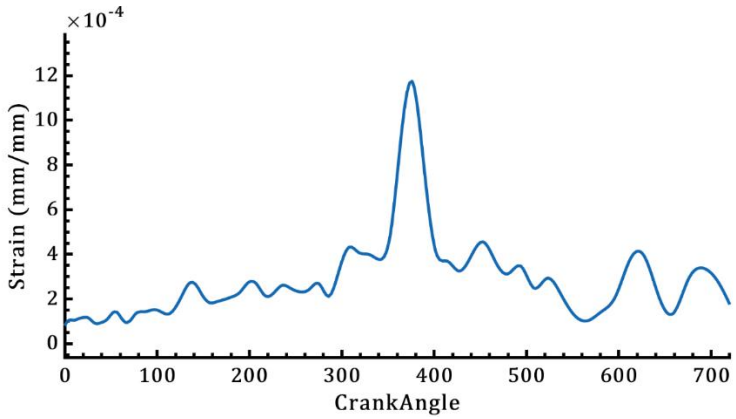

Fig. 43. Strain diagram versus crank angle for the critical piston element in the ignition phase without thermal effects.

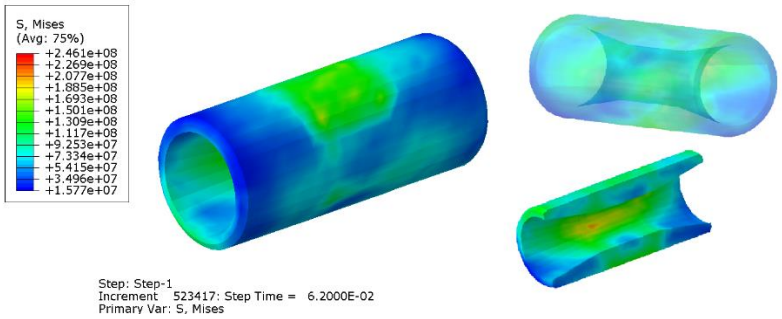

Fig. 44. Contourof maximum stress for the Gudgeon pin in the ignition phase with applied pressure on the piston crown and without considering thermal effects.

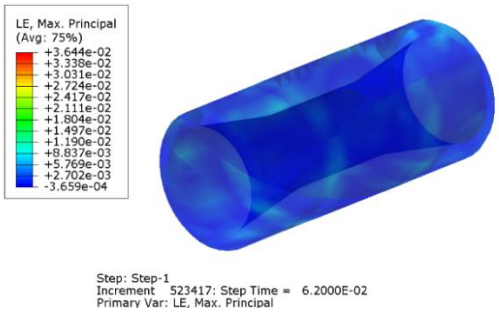

Fig. 45. Contourof maximum strain for the Gudgeon pin in the ignition phase with applied pressure on the piston crown and without considering thermal effects.

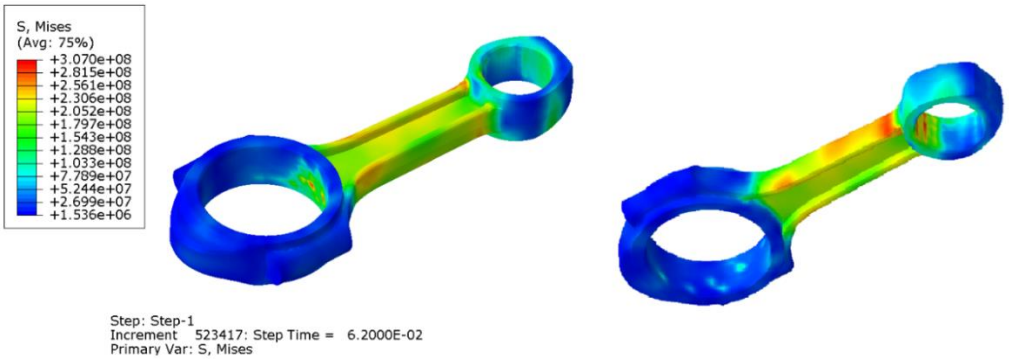

Fig. 46. Contourof maximum stress for the connecting rod in the ignition phase with applied pressure on the piston crown and without considering thermal effects.

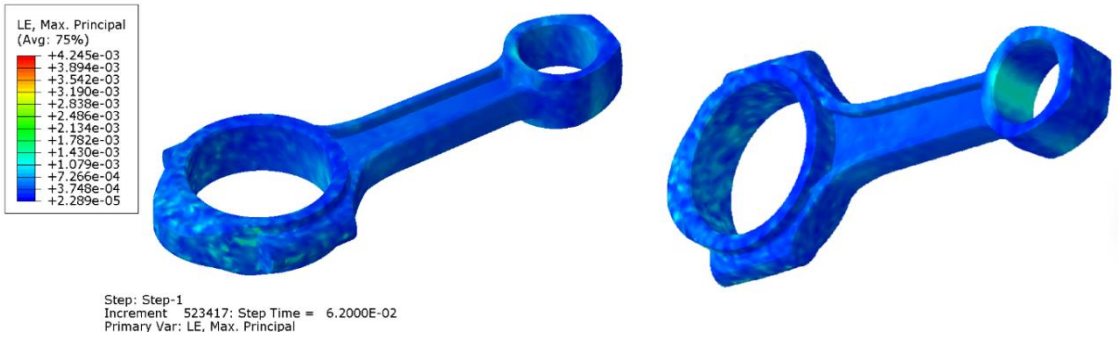

Fig. 47. Contourof maximum strain for the connecting rod in the ignition phase with applied pressure on the piston crown and without considering thermal effects.

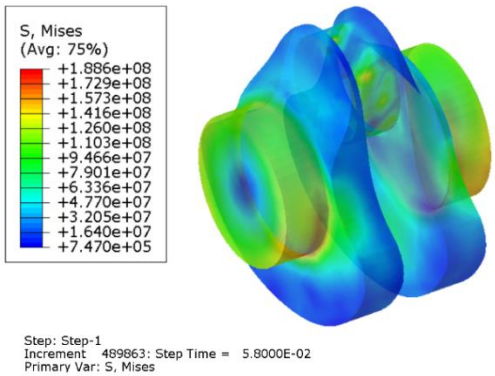

Fig. 48. Contourof maximum stress for the crankshaft in the ignition phase with applied pressure on the piston crown and without considering thermal effects.

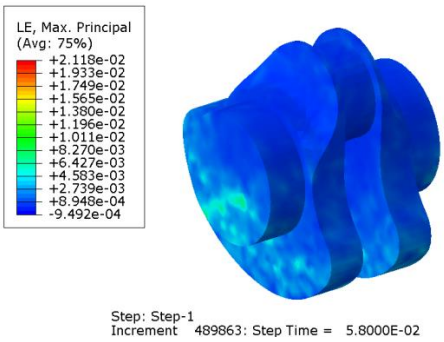

Fig. 49. Contourof maximum strain for the crankshaft in the ignition phase with applied pressure on the piston crown and without considering thermal effects.

In the first analysis, a simulation without the thermal effects of the cylinder chamber and piston crown is performed. In this case, the Mercury engine rotates at a speed of 2800 RPM, and the maximum pressure on the piston crown is 68 bar. In this analysis, the maximum stresses for the piston pin, connecting rod, and crankshaft are 189, 307, and 246 MPa, respectively. The safety factors for the critical elements, the piston pin, connecting rod, and crankshaft, are calculated as 5/6, 2/3, and 4, respectively. Considering that the maximum stress for the critical element, the piston, is 115 MPa, the safety factor for the piston is 3.

In the second analysis, thermal effects are applied to the piston crown, while the other boundary conditions remain the same as in the first analysis. This includes the rotational speed of the connecting rod at 2800 RPM and the maximum cylinder chamber pressure set to 68 bar.

4.2.2. Dynamic Simulation of Mercury Engine with Thermal Effects

Figures (50) to (65) represent contour plots of maximum stress, and strain for the piston when thermal effects are considered for the four phases: intake, compression, ignition, and exhaust.

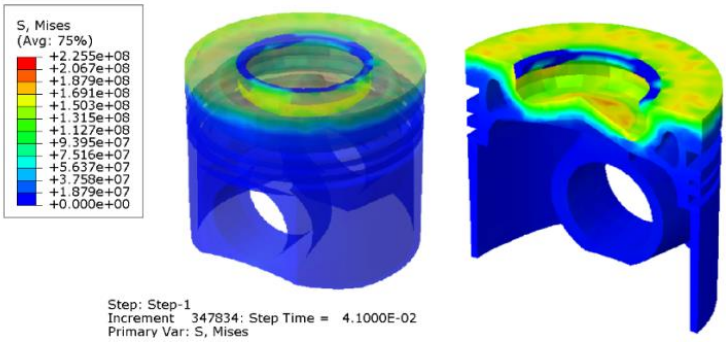

Fig. 50. Contour of maximum stress in the piston crown for the intake phase with applied pressure on the piston crown and thermal effects.

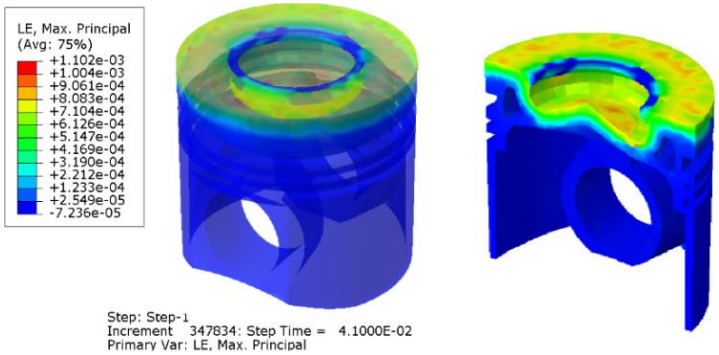

Fig. 51. Contour of maximum strain in the piston crown for the intake phase with applied pressure on the piston crown and thermal effects.

In the intake phase, the maximum stress in the piston crown is 225 MPa, which has increased more than 30 times compared to the stress in the piston crown in the first analysis without thermal effects, indicating a significant impact.

In the intake phase, the maximum stress in the notched piston crown is 36 MPa, which has increased by only 2 MPa compared to the stresses in this part of the piston in the first analysis, which was conducted without thermal effects.

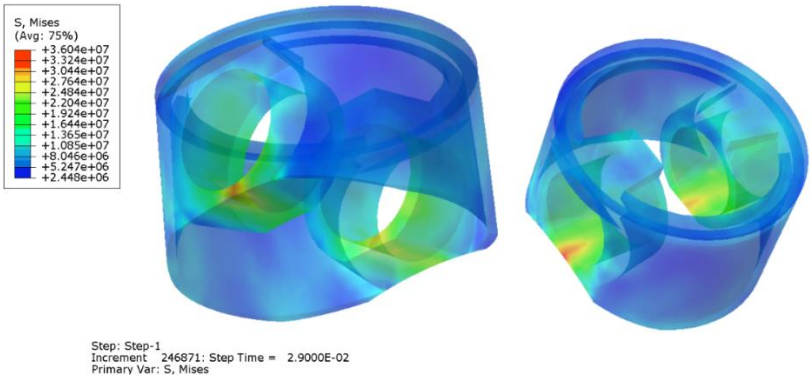

Fig. 52. Contour of maximum stress when the piston crown is notched, for the intake phase with applied pressure on the piston head and thermal effects.

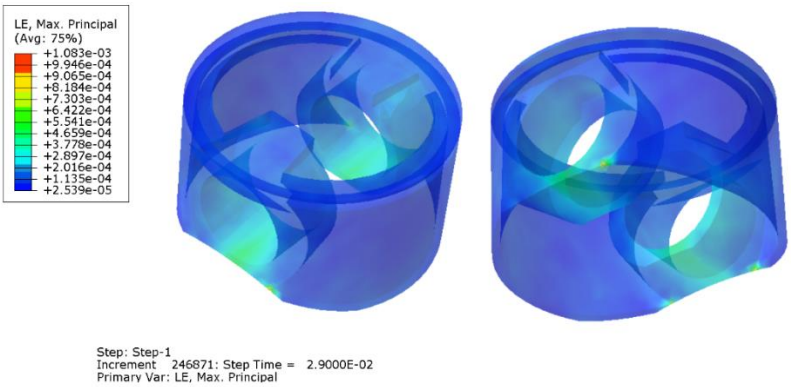

Fig. 53. Contour of maximum strain when the piston crown is notched, for the intake phase with applied pressure on the piston head and thermal effects.

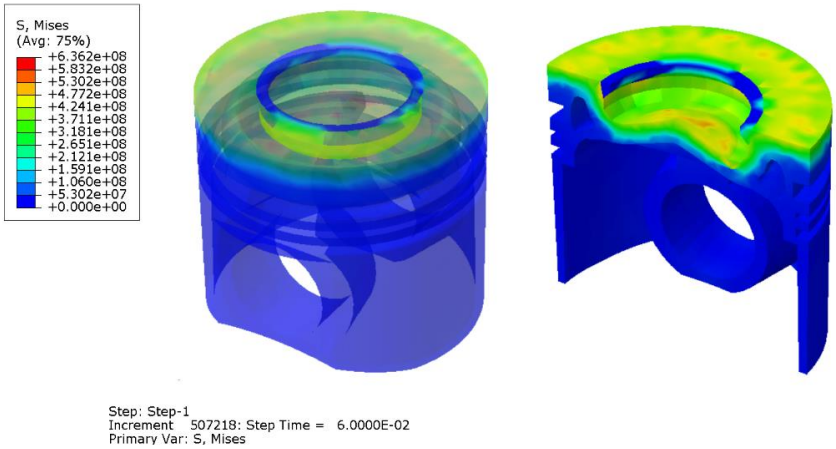

Fig. 54. Contour of maximum stress in the piston crown for the compression phase with applied pressure on the piston crown and thermal effects.

In the compression phase, the maximum stress in the piston crown is 636 MPa, which is over 42 times higher compared to the stresses in the piston crown in the first analysis without thermal effects. Additionally, the stress in the piston crown has increased nearly threefold compared to the intake phase.

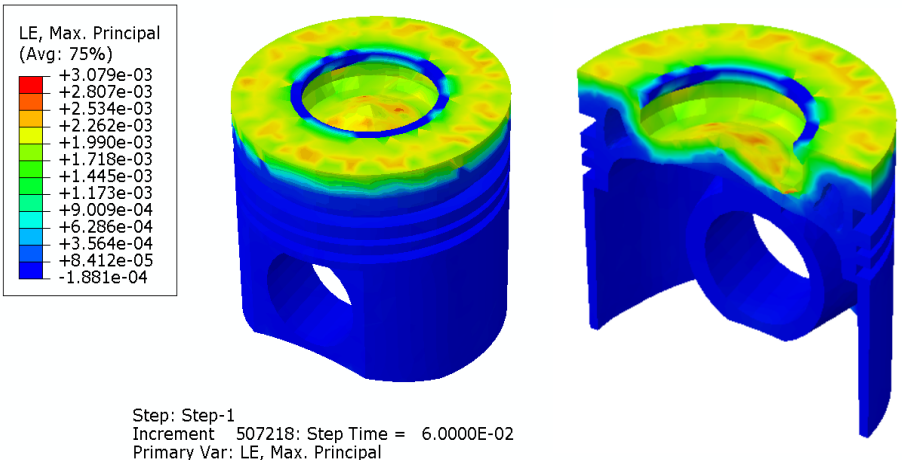

Fig. 55. Contourof maximum strain in the piston crown for the compression phase with applied pressure on the piston crown and thermal effects.

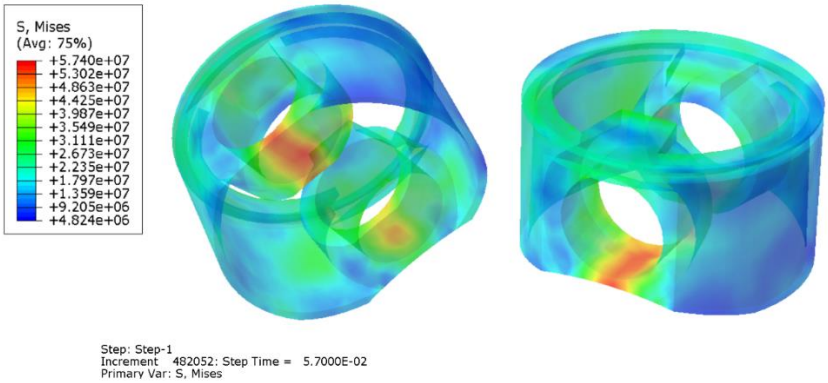

Fig. 56. Contour of maximum stress in the piston crown in a sheared state, for the compression phase with applied pressure on the piston head and thermal effects.

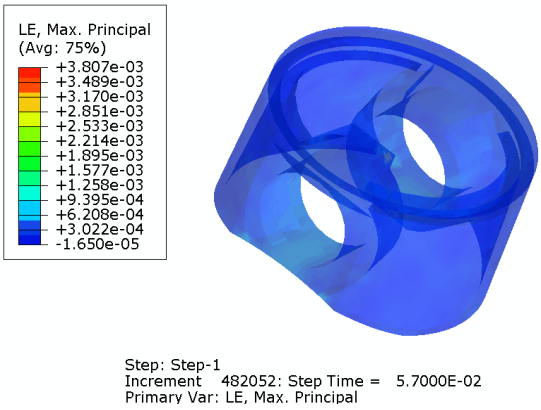

Fig. 57. Contour of maximum strain in the piston crown in a sheared state, for the compression phase with applied pressure on the piston head and thermal effects.

In the compression phase, the maximum stress in the sheared state of the piston crown is 57 MPa, which, compared to the stress in this part of the piston in the first analysis for the compression phase without thermal effects, has only increased by 11 MPa.

In the ignition phase, the maximum stress in the piston crown is 839 MPa, which is compared more than 28 times higher to the stresses in the piston crown in the first analysis without thermal effects, which is significantly noticeable. Additionally, the stress level in the piston crown has increased by 24% compared to the compression phase.

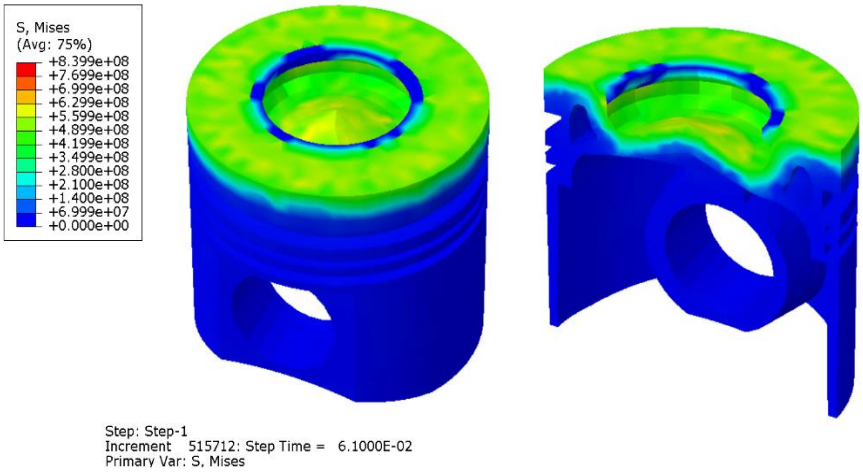

Fig. 58. Contour of maximum stress in the piston crown for the ignition phasewith applied pressure on the piston head and thermal effects.

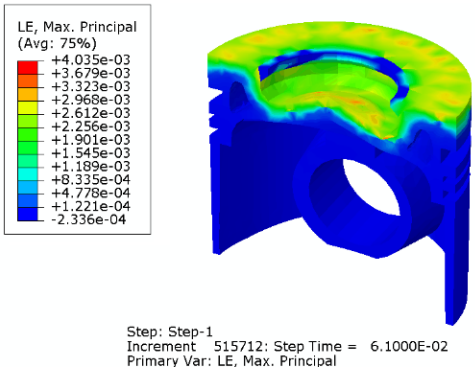

Fig. 59. Contour of maximum strain in the piston crown for the ignition phasewith applied pressure on the piston head and thermal effects.

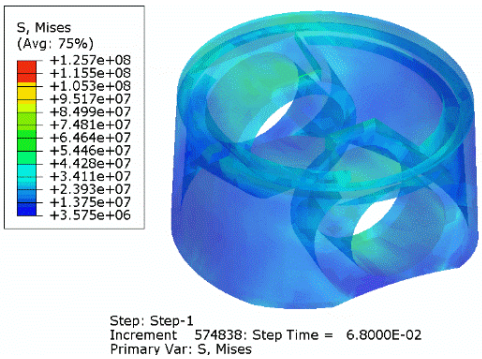

Fig. 60. Contour of maximum stress in the condition where the piston crown is notched, for the ignition phasewith applied pressure on the piston head and thermal effects.

In the ignition phase, the maximum stress in the condition where the piston crown is notched is 125 MPa, which is only 11 MPa higher compared to the stress in this part of the piston in the first analysis for the ignition phase without thermal effects.

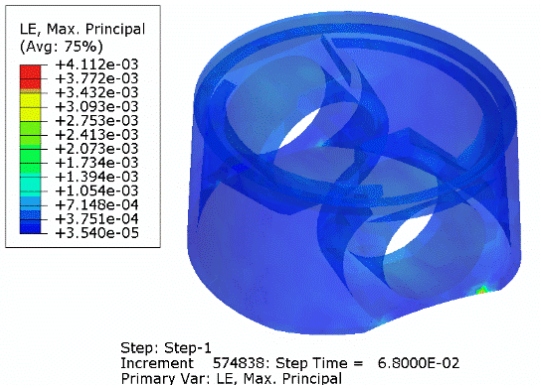

Fig. 61. Contour of maximum strain in the condition where the piston crown is notched, for the ignition phasewith applied pressure on the piston head and thermal effects.

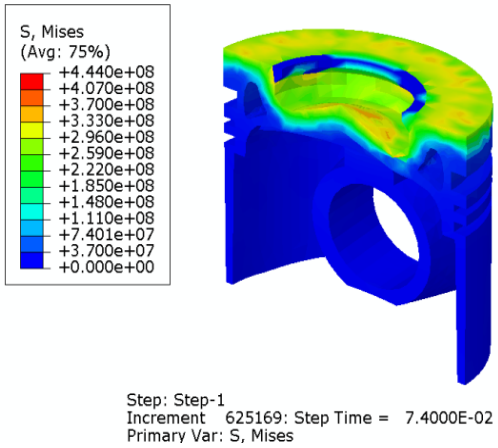

Fig. 62. Contour of maximum stress in the piston crown for the exhaust phase with applied pressure on the piston head and thermal effects.

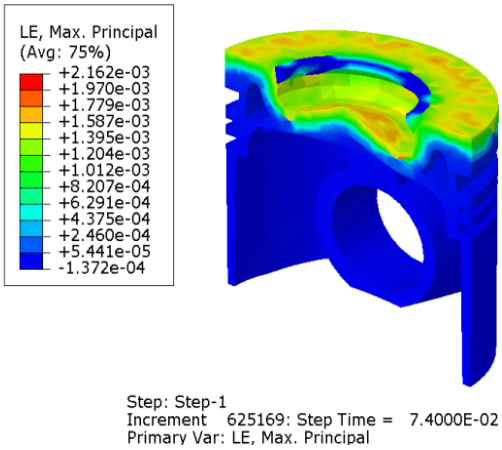

Fig. 63. Contour of maximum strain in the piston crown for the exhaust phase with applied pressure on the piston head and thermal effects.

In the exhaust phase, the maximum stress in the piston crown is 444 MPa, which is compared more than 20 times higher to the stress in the piston crown in the first analysis without thermal effects.

In the exhaust phase, the maximum stress in the condition where the piston crown is sheared is 73 MPa, which has increased by 23 MPa compared to the stresses in this part of the piston in the first analysis for the ignition phase without thermal effects.

The obtained results show that considering thermal effects on the piston crown leads to the generation of thermal stresses and a significant increase in stresses in the piston crown region. However, the thermal effects of the cylinder chamber are more pronounced in the piston crown, and in other parts of the piston, the impact is not as noticeable.

Stress, and strain diagrams for the critical element of the piston crown in the ignition phase are extracted about the crank angle, as shown in Figs. (66) and (67).

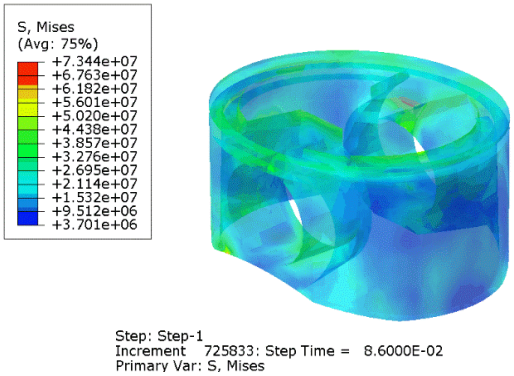

Fig. 64. Contour of maximum stress in a condition where the piston crown is sheared, for the exhaust phase with the application of pressure on the piston crown and thermal effects.

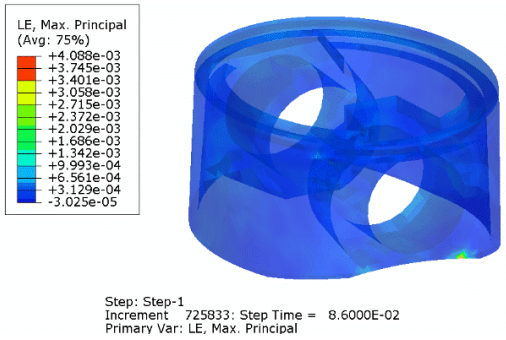

Fig. 65. Contour of maximum strain in a condition where the piston crown is sheared, for the exhaust phase with the application of pressure on the piston crown and thermal effects.

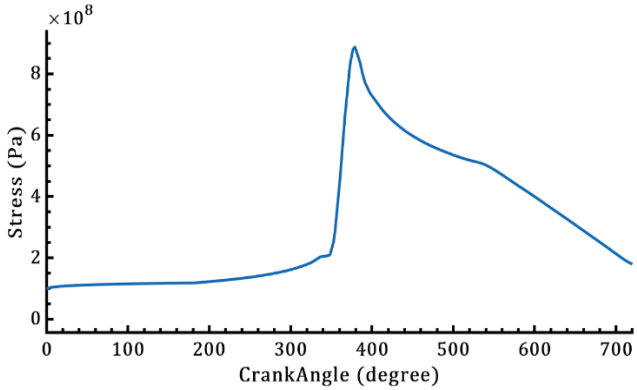

Fig. 66. Stress diagram as a function of crank angle for the critical element of the piston crown in the power phase with the application of thermal effects.

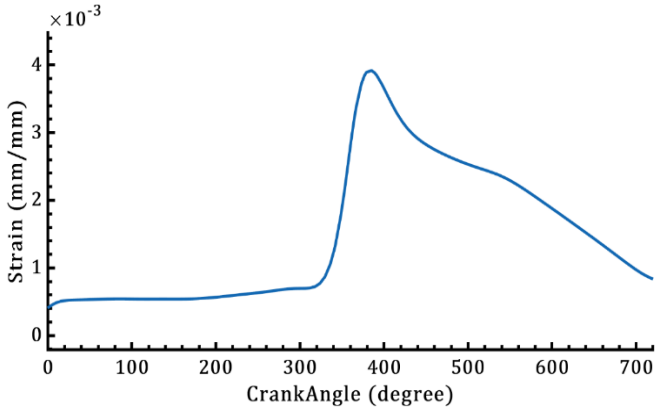

Fig. 67. Strain diagram as a function of crank angle for the critical element of the piston crown in the power phase with the application of thermal effects.

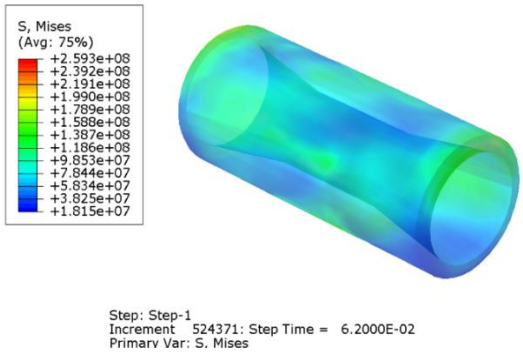

Fig. 68. Contour of maximum stress for the Gudgeon pin in the power phase with the application of pressure on the piston crown and thermal effects.

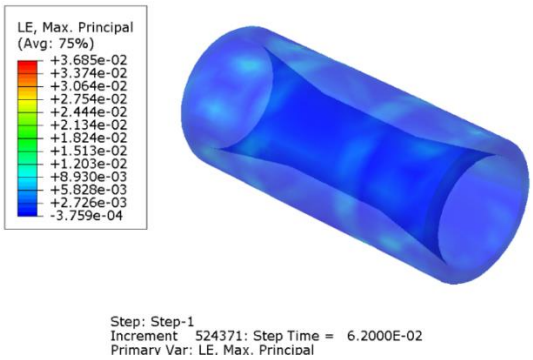

Fig. 69. Contour of maximum strain for the Gudgeon pin in the power phase with the application of pressure on the piston crown and thermal effects.

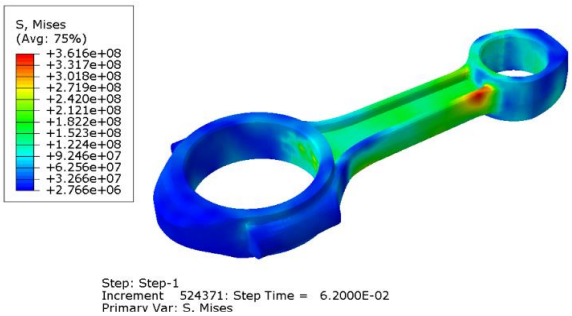

Fig. 70. Contour of maximum stress for the connecting rod in the power phase with the application of pressure on the piston crown and thermal effects.

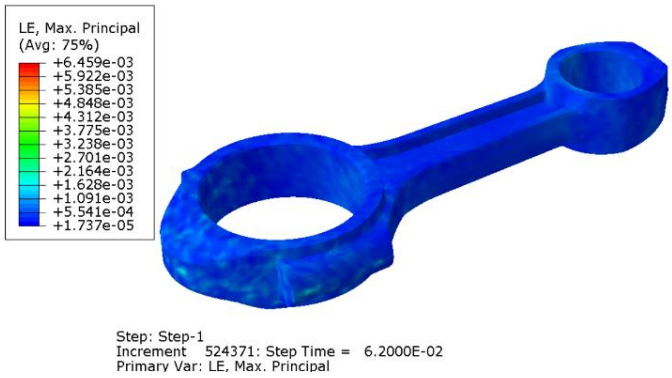

Fig. 71. Contour of maximum strain for the connecting rod in the power phase with the application of pressure on the piston crown and thermal effects.

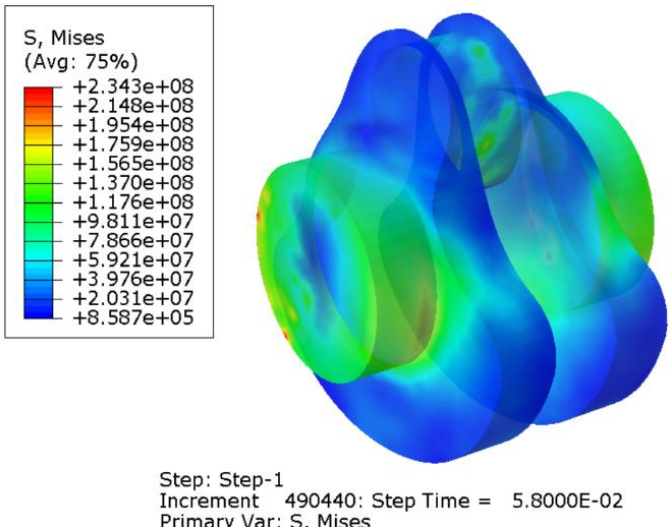

Fig. 72. Contour of maximum stress for the crankshaft in the power phase with the application of pressure on the piston crown and thermal effects.

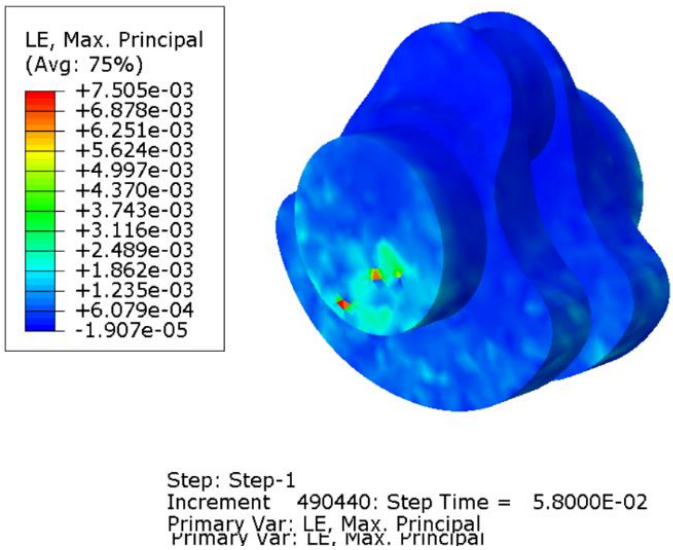

Fig. 73. Contour of maximum strain for the crankshaft in the power phase with the application of pressure on the piston crown and thermal effects.

In the second analysis with thermal effects on the cylinder chamber, the Mercury engine operates at a speed of 2800 RPM, and the maximum pressure and temperature in the cylinder chamber are 68 bar and 2700 degrees Celsius, respectively. In this analysis, the maximum stresses for the pin boss, connecting rod, and crankshaft are 259, 361, and 234 MPa, respectively. The safety factors for the critical elements, namely the pin boss, connecting rod, and crankshaft, are 4.7, 2.7, and 4, respectively, in the first analysis.

4.2.3. Investigating the Effect of Ceramic Coating on the Piston Crown on the Mechanical Behavior of a Mercury Engine

By comparing the results obtained for the first and second analyses, the importance of thermal stresses and the significant effect of thermal loads on the stresses in the piston crown are more noticeable than ever. Comparative results for the first and second analyses are presented in Table (11).

Table 11. Comparative results of the first and second analyses

Piece's name	Boundary condition	Maximum tension	Crank angle in maximum tension (degree)	Critical element's position
Piston	speed 2800 RPM ، maximum pressure 68 bar	115 MPa	376.7	Piston pin hole
	speed 2800 RPM ، maximum pressure 68 bar ،maximum temperature of the cylinder compartment 2700°C	839 MPa	364.6	Piton bottom
Connecting rod	speed 2800 RPM ، maximum pressure 68 bar	307 MPa	376.7	Connecting rod handle and near the small spring
	speed 2800 RPM ، maximum pressure 68 bar ،maximum temperature of the cylinder compartment 2700°C	361MPa	376.7	Connecting rod handle and near the small spring
Gudgeon pin	speed 2800 RPM ، maximum pressure 68 bar	189MPa	376.7	The middle of the inner wall of the Gudgeon pin hole
	speed 2800 RPM ، maximum pressure 68 bar ،maximum temperature of the cylinder compartment 2700°C	259MPa	376.7	In the contact area of the piston and in the outer wall of the beginning and end of Gudgeon pin
Crankshaft	speed 2800 RPM ، maximum pressure 68 bar	246MPa	329.67	At the junction of crankshafts and fixed bearings
	speed 2800 RPM ، maximum pressure 68 bar ،maximum temperature of the cylinder compartment 2700°C	246MPa	329.67	At the junction of crankshafts and fixed bearings

According to Table 11, it can be concluded that the application of thermal loads on the piston crown results in an eightfold increase in stress values on the piston crown. However, the effect of thermal loads on other components, including the pin, connecting rod, and crankshaft, is negligible. The proposed solution in this study to reduce stress in the piston crown is to use the quenching process on the piston crown. Figures (74) to (81) show the results obtained for stress, and strain levels in the piston of the Mercury diesel engine when the quenching process is applied to the piston crown.

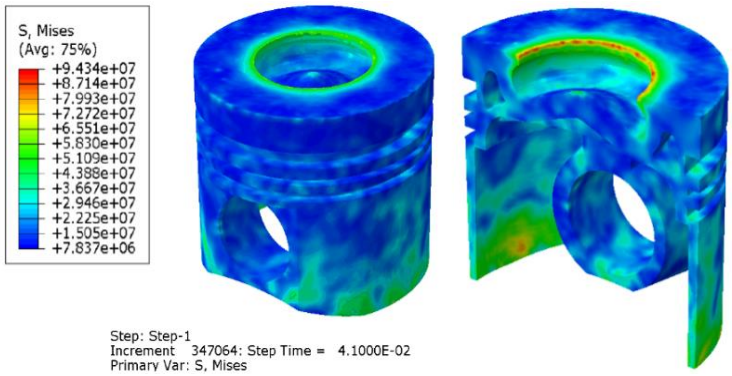

Fig. 74. Contourof maximum stress in the piston for the intake phase with applied pressure on the piston crown and thermal effects in the ceramic-coated state.

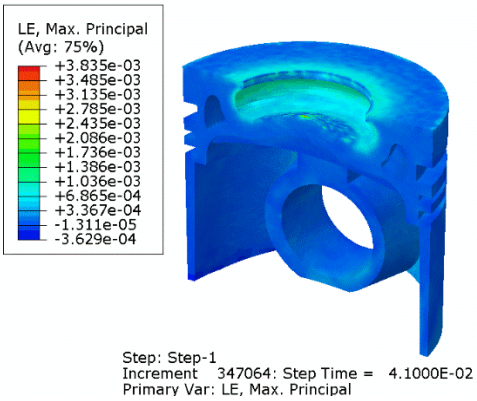

Fig. 75. Contourof maximum strain in the piston for the intake phase with applied pressure on the piston crown and thermal effects in the ceramic-coated state.

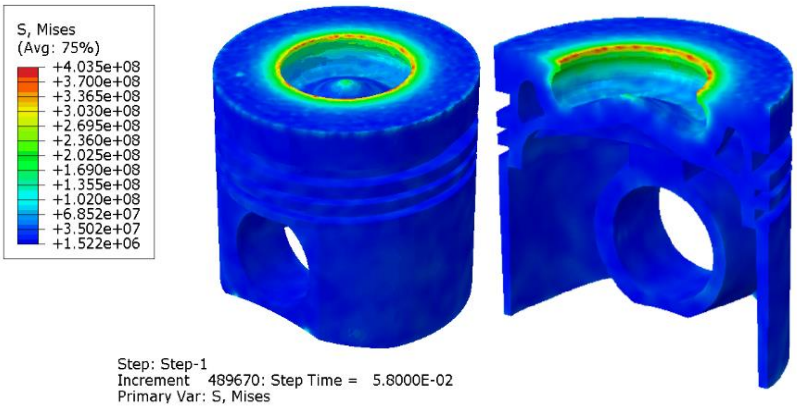

Fig. 76. Contourof maximum stress in the piston for the compression phase with applied pressure on the piston crown and thermal effects in the ceramic-coated state.

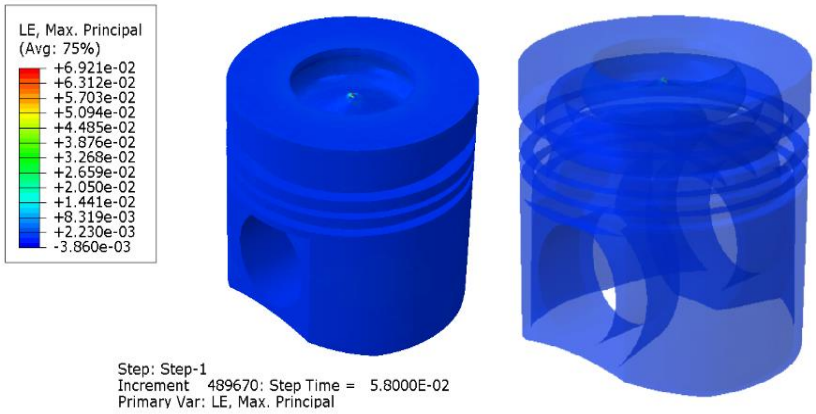

Fig. 77. Contourof maximum strain in the piston for the compression phase with applied pressure on the piston crown and thermal effects in the ceramic-coated state.

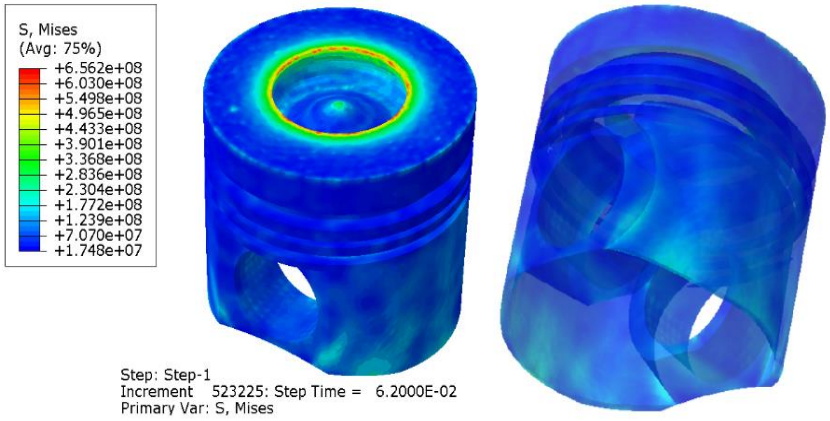

Fig. 78. Contourof maximum stress in the piston for the ignition phase with applied pressure on the piston crown and thermal effects in the ceramic-coated state.

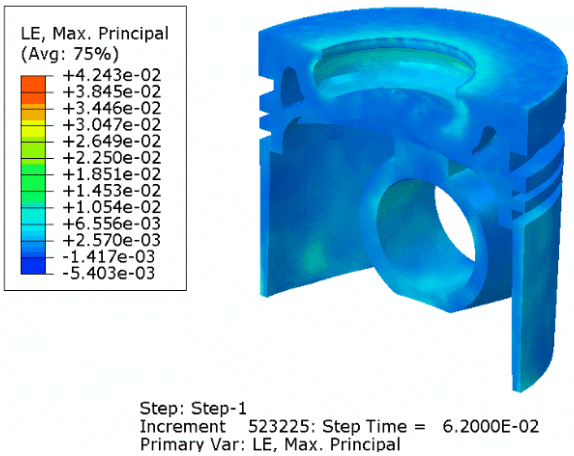

Fig. 79. Contourof maximum strain in the piston for the ignition phase with applied pressure on the piston crown and thermal effects in the ceramic-coated state.

The maximum stress on the piston crown, obtained through dynamic simulation of the mercury engine using Abaqus software and numerical analysis under operating conditions of 2800 RPM and maximum pressure of 68 bar in the cylinder chamber, considering thermal effects and a maximum temperature of 2700 degrees Celsius on the piston crown, is 656 MPa.

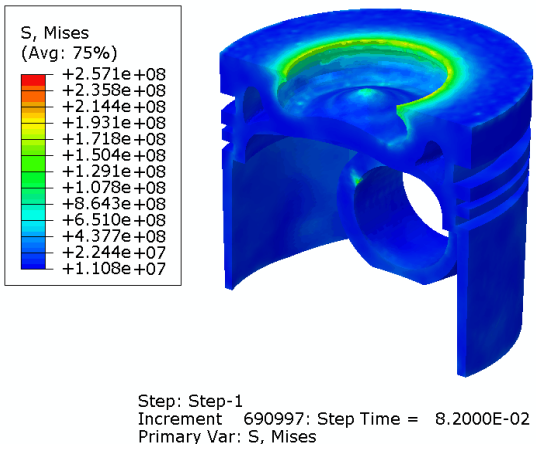

Fig. 80. Contourof maximum stress in the piston for the exhaust phase with applied pressure on the piston crown and thermal effects in the ceramic-coated state.

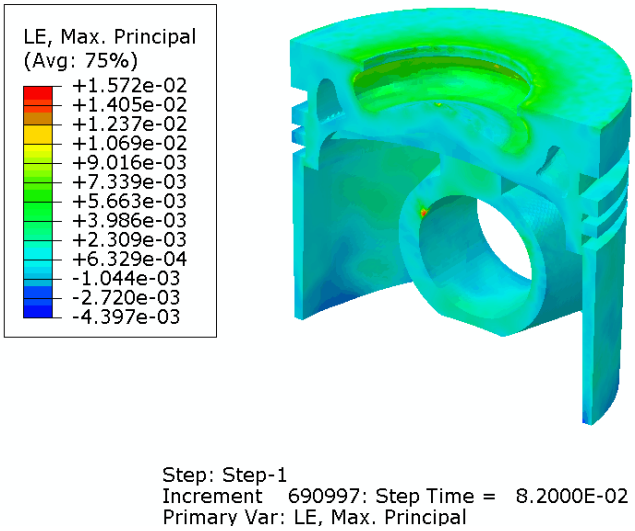

Fig. 81. Contourof maximum strain in the piston for the exhaust phase with applied pressure on the piston crown and thermal effects in the ceramic-coated state.

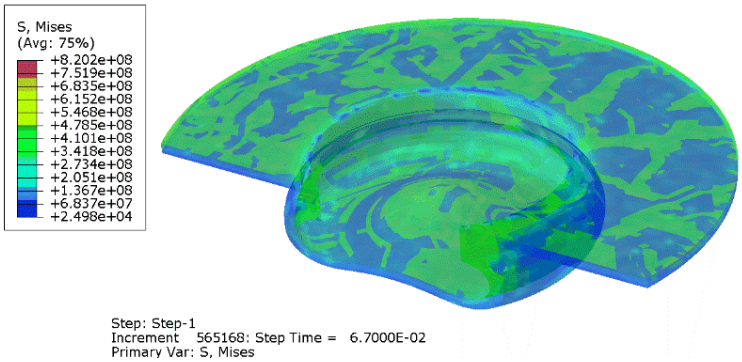

Fig. 82. Contourof maximum stress in the ceramic coating for the combustion phase.

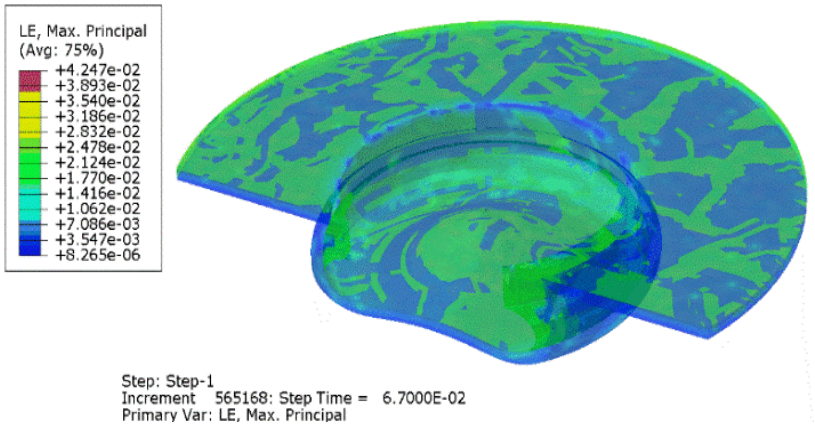

Fig. 83. Contourof maximum strain in the ceramic coating for the combustion phase.

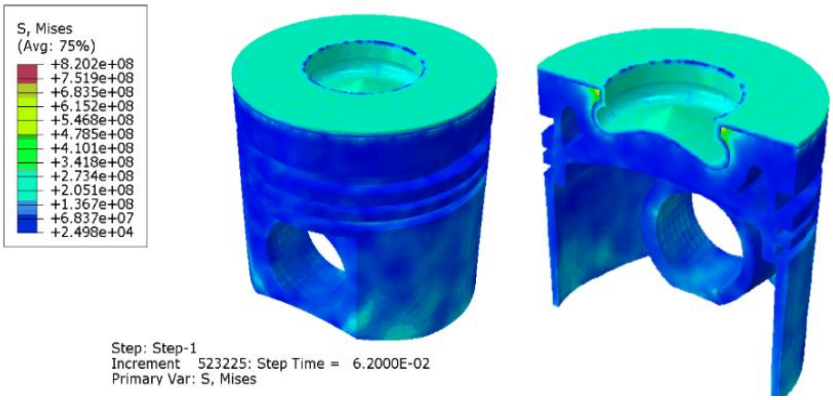

Fig. 84. Contourof maximum stress in the piston and ceramic coating for the combustion phase.

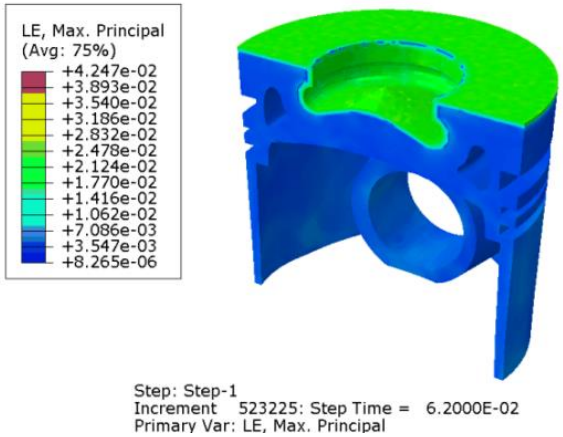

Fig. 85. Figure 49: Contourof maximum strain in the piston and ceramic coating for the combustion phase.

Table 12: Results of maximum stress in the piston for four phases: intake, compression, ignition, and exhaust, for the ceramic-coated piston and the piston without ceramic coating.

Table 13: Reduction in Stress and Increase in Safety Factor for Critical Element (Crown Piston) in the Phases of Intake, Compression, Combustion, and Exhaust by Applying Ceramic Coating (La2Ce2o7) to the Piston Crown.

Table 12. Comparison of Maximum Stress in Piston with Ceramic Coating and Without Coating

Piston with ceramic coating		
Boundary condition	**four-stroke diesel engine cycle phases**	**Maximum pressure**
Speed 2800RPM, Maximum pressure 68 bar Maximum tempreture2700°C	intake	94 MPa
	compression	403 MPa
	ignition	650 MPa
	exhaust	257 MPa
Piston without coating		
Boundary condition	**four-stroke diesel engine cycle phases**	**Maximum pressure**
Speed 2800RPM, Maximum pressure 68 bar Maximum tempreture2700°C	intake	225 MPa
	compression	636 Mpa
	ignition	840 Mpa
	exhaust	444 MPa

Table 13. Percentage Reduction in Maximum Stress and Increase in Safety Factor for Mercury Engine with Ceramic Coated Piston

Increasing the confidence factor for the critical element (%)	Reduction of maximum stress (%)	four-stroke diesel engine cycle phases
140	58	intake
60	36	compression
23	22.6	ignition
42	42.1	exhaust

5. Conclusion

Considering the obtained results, it is observed that taking thermal effects into account in the piston crown leads to the generation of thermal stresses and a significant increase in stresses in the piston crown region. However, the influence of the cylinder chamber temperature is more prominent in the piston crown, with less noticeable effects in other parts of the piston. By comparing the results obtained from the first and second analyses, the importance of thermal stresses and the significant impact of thermal loads on piston crown stresses are more evident. The comparative results of the first and second analyses are presented in Table (14).

According to Table 14, it can be concluded that the application of thermal loads on the piston crown increases the stress level in the piston crown by 8 times, while the effect of thermal loads on other components, including the pin, connecting rod, and crankshaft, is negligible. The proposed solution in this study to reduce stress in the piston crown is to use the quenching process on the piston crown. By performing the quenching process with ceramic coating (La2Ce2o7) on the piston crown, the stress level has been significantly reduced in all phases. The reduction in stress for the critical component in the phases of compression, ignition, and exhaust, and the increase in the safety factor for the piston crown are presented in the obtained results.

According to the results obtained in Table 15, it can be concluded that the quenching process in the piston crown with a ceramic material reduces the maximum stress by an average of 40% for the critical components in the four phases of compression, compression, ignition, and exhaust. As a result, it leads to a 23% increase in the safety factor for the critical component in the ignition phase

Table 14. Comparative Results of the First and Second Analyses

Piece's name	Boundary condition	Maximum tension	Crank angle in maximum tension (degree)	Critical element's position
Piston	speed 2800 RPM ،maximum pressure 68 bar	115 MPa	376.7	Piston pin hole
	speed Fig. 73. RPM ،maximum pressure 68 bar ،maximum temperature of the cylinder compartment 2700°C	839 MPa	364.6	Piton bottom
Connecting rod	speed 2800 RPM ،maximum pressure 68 bar	307 MPa	376.7	Connecting rod handle and near the small spring
	speed 2800 RPM ،maximum pressure 68 bar ،maximum temperature of the cylinder compartment 2700°C	361MPa	376.7	Connecting rod handle and near the small spring
Gudgeon pin	speed 2800 RPM ،maximum pressure 68 bar	189MPa	376.7	The middle of the inner wall of the Gudgeon pin hole
	speed 2800 RPM ،maximum pressure 68 bar ،maximum temperature of the cylinder compartment 2700°C	259MPa	376.7	In the contact area of the piston and in the outer wall of the beginning and end of Gudgeon pin
Crankshaft	speed 2800 RPM ،maximum pressure 68 bar	246MPa	329.67	At the junction of crankshafts and fixed bearings
	speed 2800 RPM ،maximum pressure 68 bar ،maximum temperature of the cylinder compartment 2700°C	246MPa	329.67	At the junction of crankshafts and fixed bearings

Table 15. Percentage Reduction in Maximum Stress and Increase in Safety Factor for Mercury Engine with Ceramic-Coated Piston Material

Increasing the confidence factor for the critical element (%)	Reduction of maximum stress (%)	four-stroke diesel engine cycle phases
140	58	intake
60	36	compression
23	22.6	ignition
42	42.1	exhaust

References

[1] Gupta HN. Fundamentals of internal combustion engines. PHI Learning Pvt. Ltd; 2012.

[2] Wanli Y, et al. Simulation of transient heat transfer for coupling 3-D moving component system within internal combustion chamber. SAE Technical Paper; 2003.

[3] Harigaya Y, Toda F, Suzuki M. Local heat transfer on a combustion chamber wall of a spark-ignition engine. SAE Trans. 1993; p. 1567-75.

[4] Gots A, Klevtsov V. Causes of cracks on the edges of the combustion chamber of the diesel engine piston. IOP Conf Ser Mater Sci Eng. 2020.

[5] Zhaoju Q, et al. Diesel engine piston thermo-mechanical coupling simulation and multidisciplinary design optimization. Case Stud Therm Eng. 2019;15:100527.

[6] Singh MTSR, Yadav BK. Thermal design analysis of piston using RSM method. 2021.

[7] Ramasamy N, et al. Comparative studies of piston crown coating with YSZ and Al2O3•SiO2 on engine out responses using conventional diesel and palm oil biodiesel. Coatings. 2021;11(8):885.

[8] Margot X, Escalona-Cornejo JE, Bianco A. Development of a novel numerical methodology for the assessment of insulating coating performance in internal combustion engines. SAE Tech Pap. 2021; p. 1-14.

[9] Gangula VR, Gopal GRN, Tarigonda H. Investigation on different thermal barrier-coated piston engines using Mahua biodiesel. J Inst Eng India Ser C. 2021;102:131-44.

[10] Reddy GV, Rasu NG, Prasad TH. Analysis of performance and emission characteristics of TBC coated low heat rejection engine. Int J Ambient Energy. 2021;42(7):808-15.

[11] Balaji SA, Saranya S. Study of combustion characteristics on single cylinder direct injection diesel engine with plasma and HVOF coated ceramic powders on piston crown. Mater Today Proc. 2020;33:989-94.

[12] Gehlot R, Tripathi B. Thermal analysis of holes created on ceramic coating for diesel engine piston. Case Stud Therm Eng. 2016;8:291-9.

[13] Liu X, Wang Y, Liu W. Finite element analysis of thermo-mechanical conditions inside the piston of a diesel engine. Appl Therm Eng. 2017;119:312-8.

[14] Lu Y, et al. Analysis of thermal temperature fields and thermal stress under steady temperature field of diesel engine piston. Appl Therm Eng. 2017;113:796-812.

[15] Vedharaj S, et al. Experimental and finite element analysis of a coated diesel engine fueled by cashew nut shell liquid biodiesel. Exp Therm Fluid Sci. 2014;53:259-68.

[16] Buyukkaya E, Cerit M. Thermal analysis of a ceramic coating diesel engine piston using 3-D finite element method. Surf Coat Technol. 2007;202(2):398-402.

[17] Witek L, Zelek P. Stress and failure analysis of the connecting rod of diesel engine. Eng Fail Anal. 2019;97:374-82.

[18] Choubey N, et al. Thermal analysis on two wheeler piston with different materials by using FEA method. Int J Nonlinear Anal Appl. 2022;13(Special Issue for selected papers of ICDACT-2021):147-55.

[19] Hanza SS, et al. Corrosion behaviour of tempered 42CrMo4 steel. Mater Technol. 2021;55(3):427–33.

[20] Sharma JK, et al. Finite element modelling of Lanthanum Cerate (La2Ce2O7) coated piston used in a diesel engine. Case Stud Therm Eng. 2021;25:100865.

[21] Peiyou X, et al. Influence of piston pin hole offset on cavity erosion of diesel engine cylinder liner. Eng Fail Anal. 2019;103:217-25.